STAGE DE RECHERCHE, MIP 2e ANNEE

El Niño teleconnections in the Northern Tropical Atlantic Ocean

Téléconnexions d'El Niño dans l'Océan Atlantique Tropical Nord

Pierre Labarbe

February-July 2003

Contact :
Boris Dewitte
IRD de Nouméa
Laboratoire d'Océanographie Physique
BP A5
98848 Nouméa cedex
Nouvelle Calédonie
boris.dewitte@noumea.ird.nc

Institut de recherche pour le développement

ABSTRACT

ENSO (El Niño Southern Oscillation) is the strongest and most coherent climate event existing in both the ocean and the atmosphere at interannual timescales (periods longer than one year). A great deal of research has already been done on this phenomenon, and it has already been suggested that ENSO has not only impacts over the Tropical Pacific Ocean, but also over remote regions. In particular, a large part of the sea surface temperature (SST) anomalies that occur in the Northern Tropical Atlantic (NTA) Ocean are linked to El Niño/La Niña events.

In this study, we document the impact of ENSO events on the NTA region, using an atmospheric general circulation model of intermediate complexity, called QTCM. We also test the ability of QTCM to reproduce the observed variability with regards to the tropical teleconnections between the Pacific and the Atlantic.

We first compare to observations QTCM outputs from a standard run forced by observed SST. Experiments with specific regional forcings are also carried out, as well as sensitivity tests to different parameter modifications. Our work shows that QTCM has some skills reproducing the atmospheric variability in the NTA region. In particular, it is shown that ENSO plays a large role in the warming of the waters in this region, while their cooling is more locally controlled. Some discrepancies are also found, that may rely on the use of QTCM in a forced context.

RESUME

ENSO (El Niño Southern Oscillation) est le signal le plus cohérent et le plus fort qui existe à la fois dans l'océan et dans l'atmosphère, aux échelles de temps interannuelles (périodes supérieures à 1 an). Un important travail de recherche a déjà été réalisé sur ce phénomène, et il a été suggéré que ENSO a non seulement un impact sur la région du Pacifique Tropical, mais aussi sur des zones plus éloignées. En particulier, une part non négligeable des anomalies de température de surface de la mer (SST, Sea Surface Temperature) trouvées dans l'Océan Atlantique Tropical Nord (NTA, pour Northern Tropical Atlantic), peut être attribuée aux événements El Niño ou La Niña.

Dans cette étude, nous nous intéressons à l'impact des événements ENSO sur la région NTA en utilisant un modèle atmosphérique de circulation générale de complexité intermédiaire appelé QTCM. Cette étude est également l'occasion de tester la capacité de QTCM à reproduire la variabilité observée dans les téléconnexions entre Pacifique et Atlantique.

Dans un premier temps nous comparons aux observations des sorties de QTCM issues d'une simulation standard forcée par des SST observées. Nous réalisons ensuite des expériences avec des forçages régionaux spécifiques, ainsi que des tests de sensibilités à différents changements de paramètres. Notre travail met en évidence la capacité de QTCM à reproduire la variabilité atmosphérique dans la région NTA dans une certaine mesure. Nous montrons en particulier que ENSO joue un rôle prépondérant dans le réchauffement des eaux de la région NTA, alors que leur refroidissement est quant à lui contrôlé plus localement. Des difficultés pour reproduire la variabilité observée sont également rencontrées, qui reposent probablement sur l'utilisation de QTCM dans un contexte forcé.

Contents

Introduction

At interannual timescales (i.e. at periods longer than one year), ENSO (El Niño Southern Oscillation) is the most striking event on both the atmospheric and oceanic circulation, in the Tropical Pacific. It has also strong impacts all over the world. In 1997–1998 occurred one of the most intense El Niño events. In Peru and Equator, rainfalls were up to thirty times higher than usual, causing destructive flooding. On the contrary, on the other side of the Pacific Ocean, anomalous droughts caused devastating forest fires in Indonesia. During an El Niño event, marine ecosystems are disturbed, agriculture and economies are in danger, and epidemics are eased.

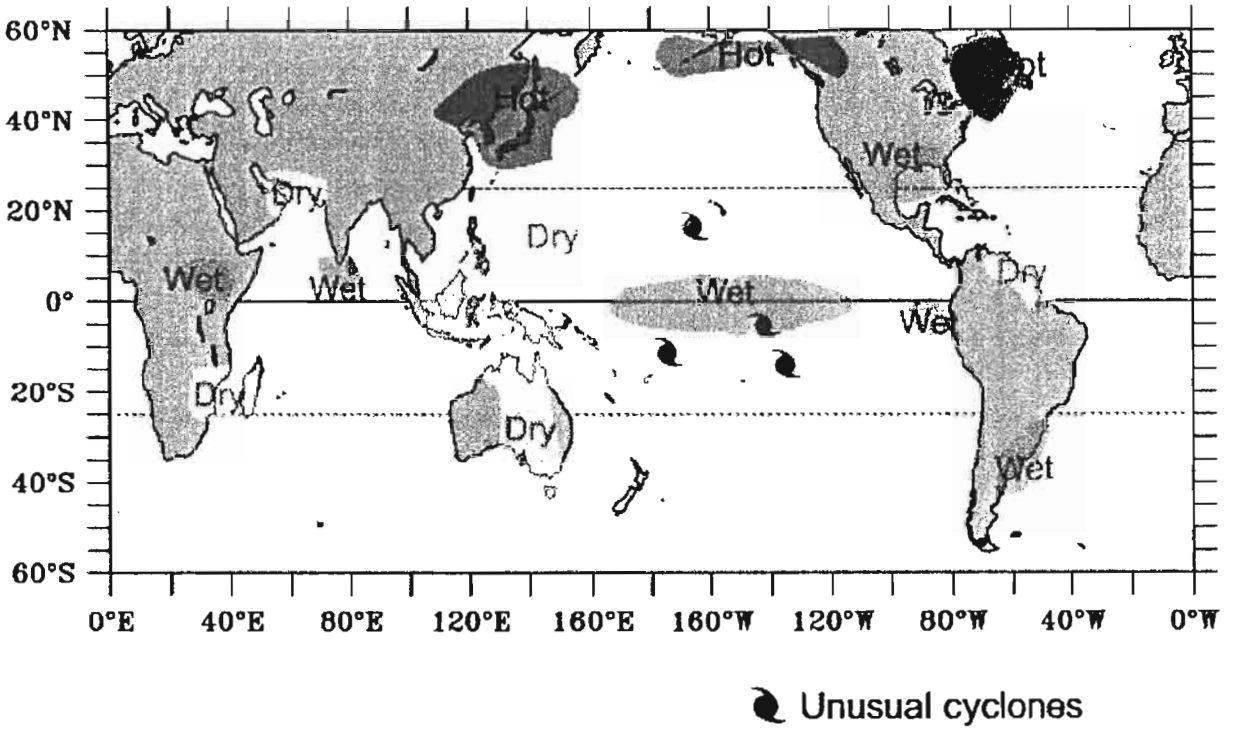

Figure 1: Main climatic anomalies during an El Niño event.

It is thus essential to understand the phenomenon in order to predict its arrival and intensity. Some countries of South America already use El Niño predictions to plan their seeds and limit the negative effects of an El Niño event. Unfortunately, ENSO is far from being understood, because it has not been studied for a long time. The knowledge of El Niño has grown with the observation network that was born in the 80's. The 1982–1983 event has indeed shown how devastating El Niño could be. A large network of 70 moorings has been deployed in the Pacific Ocean, satellites also observe the ocean, and numerical models have been developed to understand and predict ENSO events. The phenomenon is almost cyclical : there is an oscillation between «warm» (El Niño) and «cold» (La Niña) conditions in the Pacific. Unfortunately, this oscillation is not regular. The difficulty is that each El Niño event (or its contrary La Niña) is different and does not occur regularly. Moreover, a warm event is not always followed by a cold event.

Theories, in which equatorial waves play a large role, have been proposed to understand the oscillating nature of the phenomenon. The way El Niño spreads its effects to remote region is also investigated. ENSO events have main effects in the Tropical Pacific Ocean. Nevertheless, recent studies (Klein et al. [1999], Czaja et al. [2002] (hereafter KSL and CVM), Enfield and Mestas-Nuñez [2000]) have indeed shown that ENSO plays a role in the climatic variability of further regions such as the Indian Ocean, the South China Sea, or the Tropical Atlantic Ocean. This is in particular one aim of our work to document the role played by El Niño in the Northern Tropical Atlantic variability. In this study, we have used QTCM, an atmospheric general circulation model of intermediate complexity. Our purpose was also to test how the model reproduces the observed variability, regarding the links, called «teleconnections», between the

Atlantic and the Pacific. The model was designed in particular to simulate large scale circulation, and is well adapted to the equatorial variability (Neelin and Zeng [2000], Zeng et al. [2000]). But the ability of QTCM to simulate variability at higher latitudes was not well documented yet.

We first illustrate some aspects and consequences of ENSO, and sum up the theories explaining the oscillatory nature of ENSO. We then present the QTCM model, and our methodology. In section 3, we present and discuss the main results of our work.

1 El Niño and the Southern Oscillation

1.1 Glossary

Some notions and acronyms often used in climatology are needed to understand what will follow. They are defined below.

- **baroclinic** : something that is function of the pressure.
- **down/upwelling** : vertical down/up going flow of water.
- **ENSO** : El Niño Southern Oscillation. Main climatic pattern in the Pacific, at interannual (see below) timescales. The phenomenon known as «El Niño» is linked to the «Southern Oscillation», an oscillation in atmospheric pressure between the western and the eastern/central Pacific. The succession of «warm» and «cold» conditions in the Tropical Pacific Ocean and this atmospheric oscilation are part of the same climatic phenomenon, that couples atmosphere and ocean. Many indices allow to detect the occurrence of El Niño / La Niña events. Among these, the most commonly used index is called the Southern Oscillation Index (or the SOI). It is defined as a normalized atmospheric sea level pressure difference between Darwin (Australia) and Tahiti (French Polynesia).

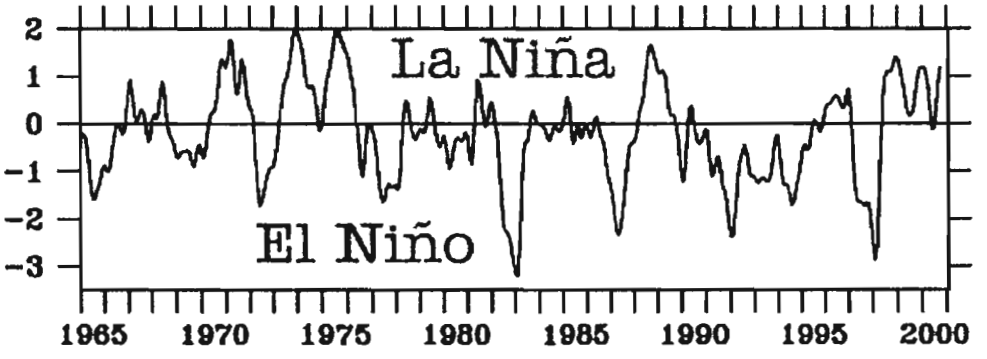

Figure 1.1: The Southern Oscillation Index over 1965–2000

When the SOI is negative (e.g., 1982/1983, 1986/1987, 1992/1993, 1997/1998) the tropical Pacific is under the influence of El Niño, when it is positive (e.g., 1973, 1975, 1988/1989, 1998/2001) it is under the influence of La Niña.

- **interannual** (timescales, or variability) : involve period greater than one year
- **intraseasonal** (timescales, or variability): involve period shorter than one year
- **NAO** : North Atlantic Oscillation. Main climatic variability pattern around the North Atlantic basin. The associated index is defined as the normalized december-march average sea level pressure anomalies between Lisbon and Stykkisholmur. It has to be related to the zone of high pressure in the Azores, that can be wether strengthened (positive NAO) or weakened (negative NAO).
- **NTA** : Northern Tropical Atlantic. Region located between 5°N–25°N and 60°W–20°W.
- **QTCM** : The Neelin an Zeng Quasi-equilibrium Tropical Circulation Model.
- **SST** : Sea Surface Temperature.
- **Sverdrup transport** : oceanic transport induced by wind stress curl.
- **teleconnections** (El Niño or ENSO teleconnections): links between ENSO and the climatic variability in those remote regions.
- **thermocline** : the sea temperature strongly decreases in the equatorial Pacific at depths of the order of 100m. The line between warm and cold water is called thermocline. The depth of the thermocline around the equator is conversely proportional to the sea level.

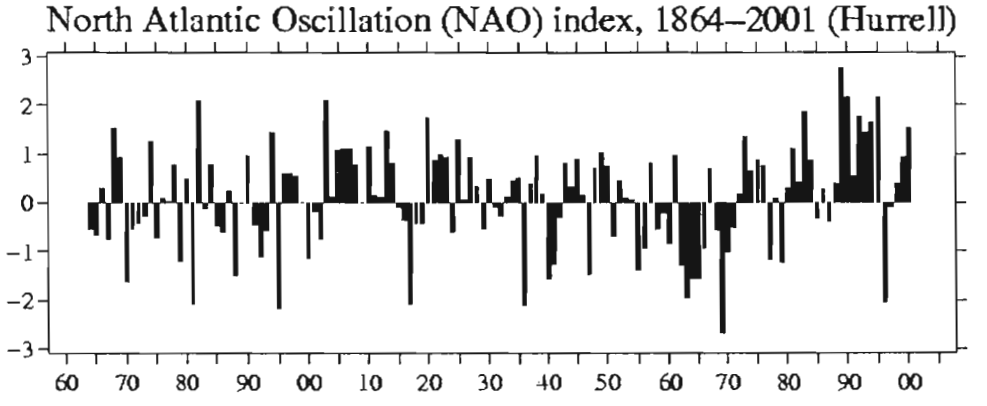

Figure 1.2: The NAO index over 1864–2001.

- **trade winds** : «Alizés» in French. Regular winds blowing from the East in the Tropics.
- **Warm Pool** : the world warmest sea waters are found in the Western Equatorial Pacific. Its location depends on the definitions : between 120°E and 180°E, and between 5/10°N and 5/10°S. Mean temperatures are around or higher than 29°C in this region (see fig. 1.4).
- **zonal** : direction parallel to the equator

1.2 The Tropical Pacific

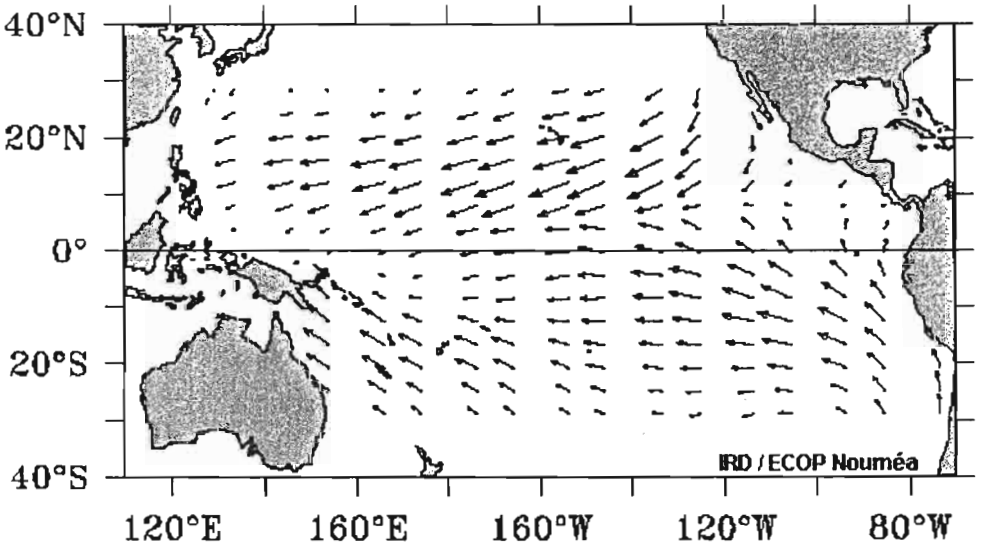

Figure 1.3: Mean surface wind field in the Pacific

The warmest waters are found in the tropical band, because solar beams strike this region perpendicularly. Due to the rotation of the Earth, in «standard» (or «mean») conditions, the trade winds blow from east to west in this region (see figure 1.3). They «push» the warm waters of the Tropical Pacific towards the West, thus creating the «Warm Pool» (see figure 1.4 and 1.5). Warm air is rising over the Warm Pool, creating a low pressure zone that attracts in turn the trade winds from the East. In parallel, the trade winds and the inversion of the Coriolis force create an equatorial upwelling on the east (not as well observed in the west because of the warm waters). This upwelling brings cold waters at the surface. The Eastern Tropical Pacific is thus colder than the Western Pacific. This difference of temperature

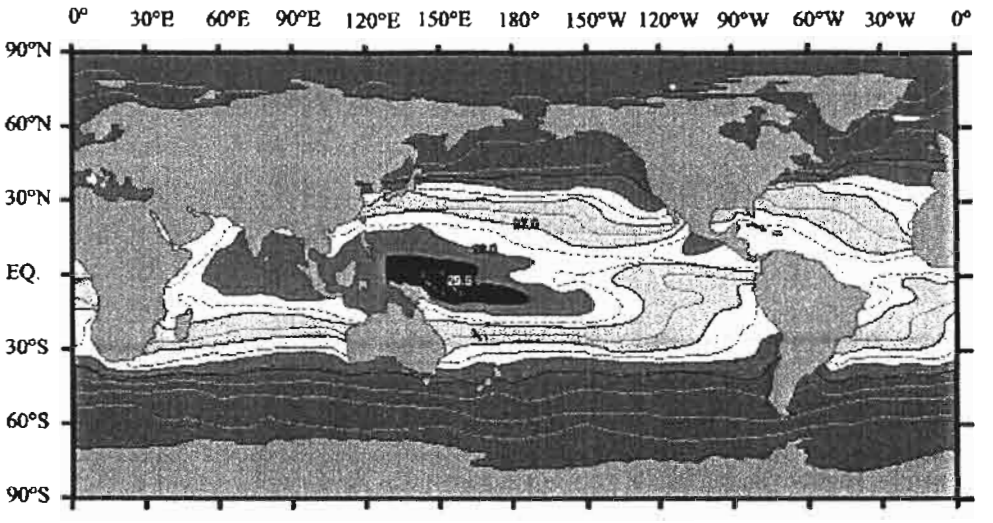

Figure 1.4: Mean sea surface temperature

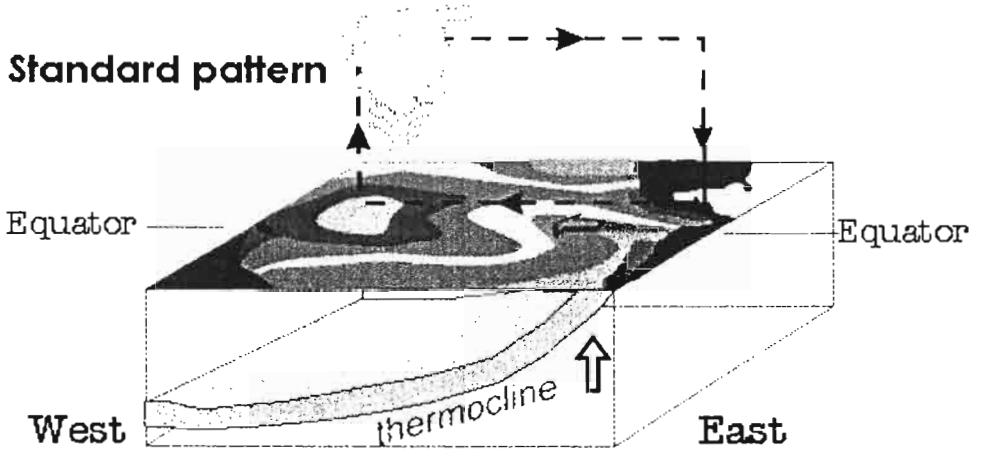

Figure 1.5: «Standard» conditions in the Tropical Pacific.

between east and west maintains the trade winds (more details on the convective «Walker» cells further). Note that, during «normal» conditions, the thermocline (line under which the sea temperature strongly decreases) is deeper on the West (about 180m) than on the East (around 70m). On the contrary, because warm water is less dense than cold water, the sea level is higher on the West. It will be seen further that the thermocline depth plays a role during ENSO events.

1.3 What happens during an El Niño

Every 2 to 7 years, the equilibrium described above is strongly disrupted. At first, a warming of the waters of several degrees was observed along the coasts of Equator and Peru. As the phenomenon occurs around December, it was called by people of Peru «El Niño », as a reference to the birth of Jesus. Then this warming was also been observed in the center of the basin. In parallel, it was seen that when the atmospheric pressure was anomalous low in Tahiti, it was abnormally high in Darwin (Australia) and *vice-versa*. This phenomenon is called the «Southern Oscillation». These anomalies are part of the same phenomenon, coupling ocean and atmosphere variability. It is now called ENSO, for El Niño / Southern oscillation.

At the early stage of an El Niño event, a weakening of the trade winds is observed over the Warm Pool (see fig. 1.6). Westerlies (winds blowing toward the east), that generally last 8 to 15 days, are even

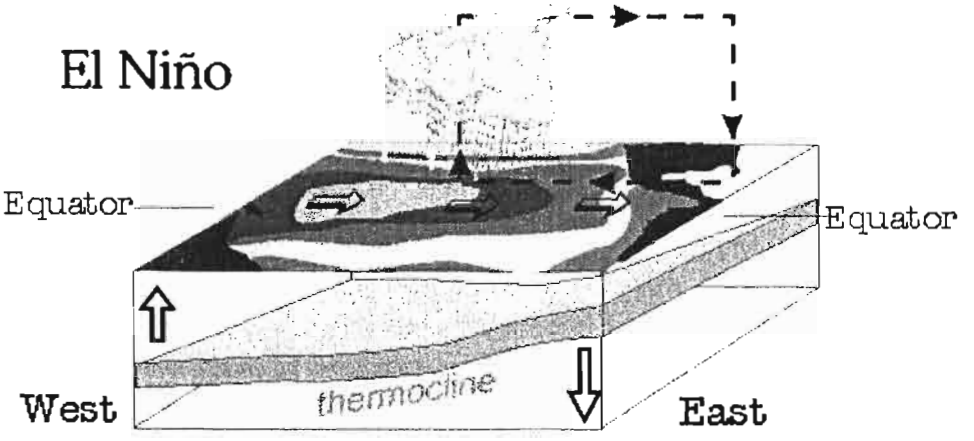

Figure 1.6: «Warm» conditions in the Tropical Pacific, found during an El Niño event.

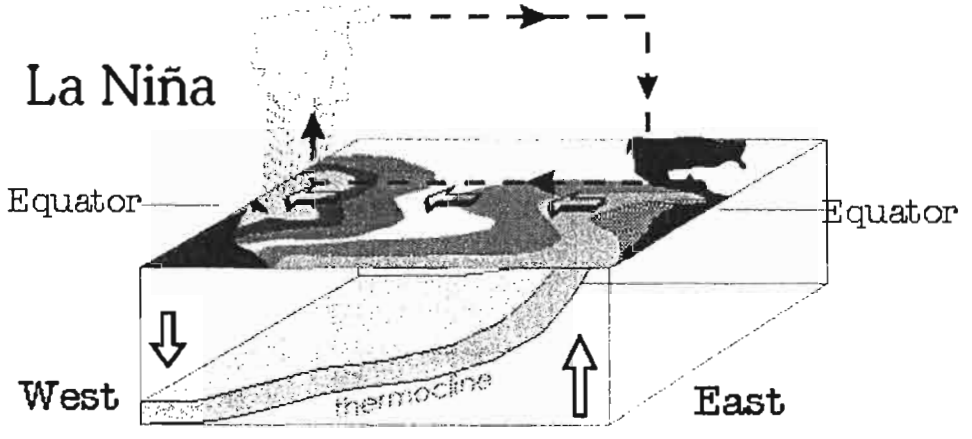

Figure 1.7: «Cold» conditions in the Tropical Pacific, found during an La Niña event.

found. It lowers the thermocline on the East and allows the warm waters to spread to the East. As the center of the warm pool is moving toward the center of the Pacific ocean, the whole convective system is disrupted. The equatorial «Walker» cell is altered, resulting in a weakening of the trade winds. It is not clear which of the moving of the warm waters or the weakening of the trade winds comes at first. What is sure is that an El Niño is slowly built and results in a succession of small complementary phenomenons that brick by brick make the anomaly.

As the convective cells are altered, there are less precipitations in the West, and Australia and Indonesia suffer from droughts. On the contrary, it rains abnormally more on the East. The thermocline is deeper and the water warmer on the East. The upwelling is weaker than usual, and brings less nutriments, resulting in marine ecosystem disturbances. This has in turn dramatic consequences on the south American fisheries. Moreover, the modification of the convective cells spreads the effects of El Niño to remote oceans (see further).

A «warm» event is often followed by a «cold» event called La Niña, which is the opposite of El Niño (see fig.1.7). The trade winds are strengthened, which pushes the warm waters more on the West, and brings more cold water on the East. The quasi-succession of El Niño and La Niña events makes the phenomenon look like an oscillation.

1.4 Proposed theories for the oscillation

1.4.1 Equatorial waves

Two main kinds of equatorial waves are likely to propagate in the tropical band, across the whole Pacific Ocean : Kelvin and Rossby waves. The theories describing the oscillatory nature of ENSO relies on the propagation of such waves. Kelvin waves can propagate toward the East and cross the Pacific ocean ($v = 3m/s$ for the first baroclinic mode). Rossby waves can propagate toward the West ($v = 1m/s$ for the first baroclinic mode).

These waves are the mathematical solution to the Navier Stockes equation under certain approximations :

- the fluid is incompressible ($div(\vec{u}) = 0$).
- non linearities are negligible.
- Coriolis coefficient is a linear function of latitude.
- the average ocean stratification is only a function of depth.

The oscillation is observed for the sea level as well as the thermocline depth. When the trade winds suddenly weaken or even blow from the west over the Pacific, at the early stage of an El Niño, it creates a brutal and local disruption of the sea level and of the thermocline : when the wind decreases in the west, the sea level lowered, and the thermocline goes back up under the wind anomaly. The anomaly begins to propagate to the east as a downwelling Kelvin wave, and to the west as an upwelling Rossby wave. The effects of these waves are to lower the thermocline on the east of the Tropical Pacific, and to raise it on the west. It takes about three months for the Kelvin wave to cross the Pacific ocean.

1.4.2 Theories on the oscillatory nature of ENSO

The Tropical Pacific generally goes from «warm» conditions during an El Niño to «cold» La Niña conditions. The ENSO phenomenon can thus look like an oscillation. We present some aspects of theories that contribute to the description of this oscillation. What follows is taken from different sources mainly the PhD work done by Sophie Cravatte (Cravatte [2003]) and Gaël Alory (Alory [2002]).

1. **The delayed oscillator** :

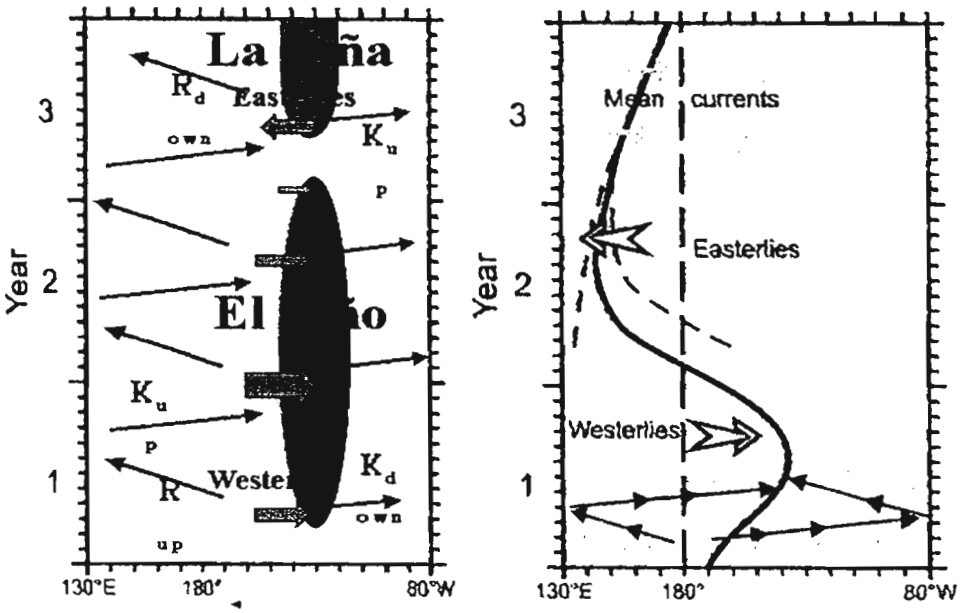

Figure 1.8: Schematic representation of the conceptual delayed (left) and advective-reflective (right) oscillators.

This is the first theory explaining the oscillatory nature of ENSO. It relies on the propagation of equatorial waves.

A weakening of the trade winds over the center of the Pacific (around 180°) creates downwelling Kelvin waves (propagating toward the east) and upwelling Rossby waves (toward the west). The Kelvin waves cause the warming of the waters in the center and the east, through the lowering of the thermocline. It also induces a weakening of the upwelling in the Eastern Pacific that usually brings cold water. In this theory, this is thus mainly a modification of the vertical advection that brings SST anomalies.

According to the theory, the Rossby waves reflects on the west of the basin. They are turned into upwelling Kelvin waves propagating toward the east. A few months later, these upwelling Kelvin waves counter the effects of the initial downwelling Kelvin waves. The thermocline goes back to its standard position in the center and the east of the Pacific. It opposes the warming of the water and may even lead to La Niña conditions.

This scenario led for the first time to the prediction of an El Niño event in 1986. The model used indeed relies on the propagation of long Rossby and Kelvin equatorial waves. However, not so good results were obtained for other ENSO events. The reflection of the waves is in fact in question. The western boundary is composed by many small islands. The ability for this boundary to reflect waves is not well known yet, because of the lack of altimetric data.

2. **The advective-reflective oscillator** :

   The theory exposed above is the most common theory used to explain the oscillatory nature of ENSO. Other theories have been proposed, such as the advective-reflective oscillator, that also relies on the propagation of equatorial waves. However, the role of the eastern boundary of the pacific is emphasized, as well as the role of zonal advection. In the theories exposed above, the warm SST anomalies in the eastern Pacific are due to the weakening of the upwelling, that is to say to vertical current anomalies. In the advective-reflective oscillator, zonal currents are associated to the equatorial waves. This currents bring the warm waters from the west. Concerning the reflection of the waves, they are also taken into account. Rossby waves are reflected on the western boundary (see fig. 1.8). The reflection of the initial Kelvin wave on the eastern boundary is also considered in this oscillator. It has the same effects than the reflection on the opposite side, resulting in the recovering of the thermocline standard position, and in possible La Niña conditions. This model thus does not recquire a perfect reflection on the western boundary.

The theories described above have common characteristics, as well as proper aspects. They all rely on a coupling between atmosphere and ocean. The main differences are found in the type of negative retroaction that makes the system go from El Niño conditions to La Niña conditions.

1.5 Irregularity of ENSO

The oscillatory nature of ENSO seems now rather well understood. However, in the theories presented above, ENSO is supposed to be cyclical, which is not true. El Niño events occur irregularly, and are not always followed by La Niña events. Moreover, every El Niño event is different in amplitude and location. Several ideas were developed to understand these irregularities or the way an ENSO event starts. The chaotic behavior of the system is in question, as well as the high frequency atmospheric forcing over the western Pacific, or the influence of lower frequencies variations.

1.5.1 Interaction with the seasonal cycle and chaos

The period of ENSO varies from 2 to 7 years. Models including the influence of the seasonal cycle managed to reproduce the frequency spectrum of ENSO. In that kind of model, a seasonal cycle is added (not taken into account in the oscillatory theories exposed below). In one of these models, the intensity of the coupling between atmosphere and ocean can be controlled through the link between wind stress and thermocline depth. Changing these parameters, the oscillation can be periodic, quasi periodic, and even chaotic.

1.5.2 High frequency and stochastic forcing

One cause for the non periodicity of ENSO may be the high frequency atmospheric forcing. It may be linked to rather coherent signal, such as the Madden-Julian Oscillation (MJO, period from 30 to 70 days). It may also be due to atmospheric noise. That kind of forcing is sometimes thought to be only responsible for a part of the non periodicity of ENSO. Nevertheless, the MJO and brief westwards winds could play a role in the beginning of the El Niño phenomenon.

1.5.3 Low frequency modulation of ENSO

Decadal variability could also play a role in the amplitude and frequency of ENSO. For example, the two probably strongest El Niño events of the century occurred in the last 20 years (1982–1983 and 1997–1998), as well as the longest (1990–1995). Moreover, at the same time period, the La Niña events are less frequent than the El Niño events. On the contrary, ENSO was rather quiet between 1950 and 1980. This may be linked to another oscillation, taking place in the Northern Pacific and which period is about 10 to 30 years (Mantua and Hare [2002]).

1.6 El Niño teleconnections

It is widely recognized that ENSO has impacts in regions far removed from the Tropical Pacific. Perhaps the most well known of these remote impact, usually designated as «teleconnections», are the changed atmospheric circulation in the northern Pacific and North America region, and the associated SST anomalies in the North Pacific. It has also been noticed that SST in the in the Indian and the Atlantic Oceans are above than normal during an El Niño (Enfield and Mestas-Nuñez [2000]). Abnormal drought are associated to these anomalies in the northeast region of Brazil and India. A number of these authors have noticed that these anomalies generally lag those in the Pacific, suggesting that the warming in the remote oceans is related to a forcing from the Pacific. Because of the presence of lands between these oceans, the explanation of these «teleconnections» may lie in the «atmospheric bridge» mechanism (Klein et al. [1999]). The SST anomalies in the tropical Pacific modify the convective cells over the Pacific Ocean. These atmospheric changes induce anomalies in the convective circulation in remote regions.

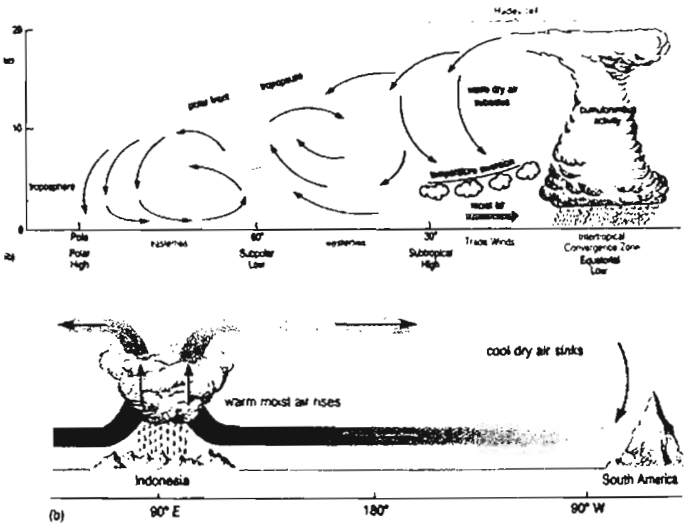

Figure 1.9: Hadley (upper pannel) and Walker (lower) cells.

During «standard» conditions, the warm waters of the Pacific are found of the west of the basin. Over this «Warm Pool», the air is warm and light, and is rising (see fig. 1.5), creating a zone of low pressures. On the contrary, on the other side of the Pacific, the air cooled during its rising, is heavier and sink over the South America, crating a high pressure zone. At the sea surface, the trade winds are generated

Figure 1.10: Schematic diagramm of modifications in the convective system during an El Niño .

given to the difference of pressure between the west and the east of the Pacific. This system of zonal convection is a «Walker» cell (see fig. 1.9) . The same kind of cell exists in the meridian directions (Hadley cells). During an El Niño , the center of the warm pool moves toward the center of the Pacific Ocean. Consequently, it modifies the position and dimension of the convective cells over the Pacific (cf fig. 1.10). These modifications have impacts on the convection system around the Pacific. It may thus brings cloud cover and wind anomalies over remote region, that, in turn, lead to SST anomalies in remote ocean. For example, in the South China Sea or in the Indian Ocean, the anomalies that are supposed to be due to ENSO are found mainly in the cloud cover. The changes in the convective cells indeed modify the zone of warm air rising and thus the zone of cloud formation. This is different in the Northern Tropical Atlantic : in this region, this is mainly the changes in wind that induce changes in heat flux toward the ocean, and thus in SST.

The difficulty in the study of remote teleconnections is the influence of other climatic patterns. For example, in the NTA region, the SST anomalies may be linked to wether ENSO or NAO (North Atlantic Oscillation) events (see glossary, section 1.1 for a definition), or the both. NAO events are indeed likely to modify the convective cells in the NTA region (see fig. 1.11).

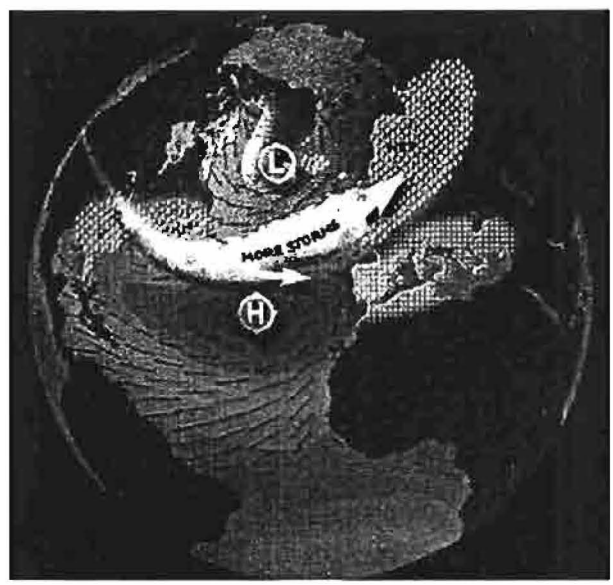

Figure 1.11: Climatic changes when the NAO index is positive

The NAO may be itself forced or at least modified by ENSO events. However, NAO events may occur without ENSO events. Other local patterns could also have an influence in the NTA region. The role played by El Niño in the NTA variability is thus not clear. This is one of the aim of this study to document this question. The use of QTCM in a forced context has enabled us to carry out experiments which aim was to isolate the influence of ENSO and local forcings.

2 Model, data description, and methodology

Since the major 1982–1993 El Niño event, the research on El Niño has grown up. A network of moorings has been installed to improve the observation of the ocean, and many oceanographic cruises have been performed. Satellites are used to improve the observations too. At the same time, numeric models have been elaborated to better understand and forecast ENSO. Nowadays, about 12 models of different complexities exist. They are coupling an oceanic model with an atmospheric model. Simple linear models are found as well as GCM (General Circulation Models) which assimilate a lot of observation, such as «Arpege», the model used by Meteo France. Hybrid models also exist, combining for instance an oceanic model of intermediate complexity, with a simple atmospheric model. The use made of these different models are not the same and do not recquire the same computing skills. The GCM need powerful computers, while it is really easy to make simulations with simple model, with a single PC.

2.1 QTCM1, version 2.3

In this study we have used the version 2.3 of QTCM (released in August 2002), the Quasi-equilibrium Tropical Circulation Model. This is an atmospheric model of intermediate complexity, which makes use of quasi-equilibrium approximations in the convective parametrization. This kind of model occupies the place between GCMs (General Circulation Model) and simple models, and is particularly well adapted to describe phenomenons in large scale convective regions such as the tropics. One of the advantages of such a model is that it is really time saving. For example, it takes less than 5 hours with a single Pentium 4 PC, for saving about 10 variables (Precipitations, wind-stress, Evaporation and other heat flux,...) over 50 years. It allowed us to carry out many experiments. This model is more complex than the models usually used to make El Niño forecasts. More physics is found in QTCM than in simple linear model. For example, intraseasonal (periods shorter than 1 year) variability can be found in this model, not like the simple models. As explained above, phenomenons occurring at these timescales such as the MJO probably play a role in the beginning of an ENSO event. The use of models such as QTCM may thus improve the ENSO previsions.

We have used the latest version of this model. In this version, climatological surface wind and stress simulation has been improved in the tropics, and are in better agreement with observations. More intraseasonal variability than in the last versions is also found, and the gross moist stability is also in better agreement with reality.

QTCM is force by SST. They can come from observations, but QTCM could be coupled to an oceanic model. The model can compute a number of atmospheric flux and momentum. For example wind speed at any surface, wind stress (N/m^2), latent (evaporation), sensible (temperature gradients), or radiative heat flux toward the ocean, precipitations, humidity, air temperature are simulated. The standard version of QTCM provides coverage from 78.75°S to 78.75°N in latitude, and coverage over all latitudes. The grid has dimensions n_x x n_y equal to 64 x 42 (spacing is 5.625 in longitude and 3.75 in latitude). The east/west boundaries are periodic, and the north/south boundaries are solid walls.

The solutions for T (Temperature), q (humidity) and $\vec{v}$ (wind speed) are searched under the form :

$$T = T_r(p) + a_1(p)T_1(x, y, t),$$
$$q = q_r(p) + b_1(p)q_1(x, y, t),$$
$$\vec{v} = \vec{v_0}(x, y, t) + V_1(p)\vec{v_1}(x, y, t)$$

Archived sample figures and the released version of the QTCM manual, with more details about the different versions of QTCM, can be found at :

`http://www.atmos.ucla.edu/~csi/QTCM`.

Other details about the earlier versions and the physics of the model can be found in Neelin and Zeng [2000] and Zeng et al. [2000].

2.2 Data and forcing

Forcing

The atmospheric model is forced by ocean sea surface temperatures (SST) provided by Reynolds and Smith [1994]. These SST combine *in situ* and satellite data analysis using optimum interpolation on a 1°x1° space grid, on the 1950-2001 period.

Observations

- **ECMWF** : We have used flux and wind stress data provided by the ECWMF reanalysis fields from January 1980 to December 1993, and the operational analysis fields from January 1994 to December 2000. Heat flux formulation is from Barnier et al. [1995].
- **TAOSTA** : Vauclair and du Penhoat [2001] have collected near surface and subsurface in situ temperature observations of the tropical Atlantic ocean between 1979 and 1998, and have built a surface and subsurface bimonthly temperature field (Tropical Atlantic Ocean Subsurface Temperature Atlas: TAOSTA : `http://medias.obs-mip.fr/taosta/`). The interpolation is based on an objective analysis method (Bretherton et al. [1976] provide a gridded data set from 70°W to 12°E and from 30°S to 30°N on a 2°x2° spatial grid with 14 vertical levels (same as those of Levitus et al. [1998])).

2.3 Methodology

We first compare our analysis from ECMWF data with earlier results of the literature (CVM, KSL). A first run with QTCM («CONTROL» run) was done over 1950–2000, which consists in forcing the model with the full SST (Reynolds and Smith [1994]) all over the model domain. Two other model runs were carried out. The first one, named «PAC», consists in running the model with the total SST over the Tropical Pacific (30°S-30°N / 100°E-80°W). Everywhere else the atmospheric model is forced with the SST seasonal cycle. The second experiment, named «ATL», consists in forcing the model with the total SST over the Northern Tropical Atlantic (2°N-30°N / 80°W-10°W), and the seasonal cycle is used everywhere else. The results of «PAC» will provide an estimate of ENSO remote forcing over the Tropical Atlantic, whereas «ATL» is supposed to isolate some of the contribution of the local forcing over the Northern Tropical Atlantic. Note however that in a forced context, forcing for «ATL» already contains variability associated to local air-sea interaction involving some contribution of the remotely forced atmospheric variability. This will have to be kept in mind when analyzing this model run.

3 Impact of the net heat flux onto the northern Tropical Atlantic

In the Northern Tropical Atlantic (NTA : 5°N–25°N, 60°W–20°W), the mechanism leading to SST anomalies is relatively well understood. Let us consider, for example, a warming of the surface waters in this area. According to CVM and KSL, changes in evaporation during the months from January to April are the main cause for these anomalies. A reduction of the trade winds, starting around January, soon leads to a reduction of the evaporation, resulting in an increase of the net heat flux (positive anomalies toward the ocean), and a warming of the surface waters. It is still not clear why there is a reduction of the trade winds. According to KSL, it could be linked to anomalous low pressures at the same period over the south-east United States, associated with the Pacific-North American (PNA) pattern, which is usually strongly correlated to the ENSO index at this period. The weakening of the Hadley cell over the Atlantic could also play a role in the weakening of the trade winds (cf. KSL).

3.1 Regressions onto the NTASST index

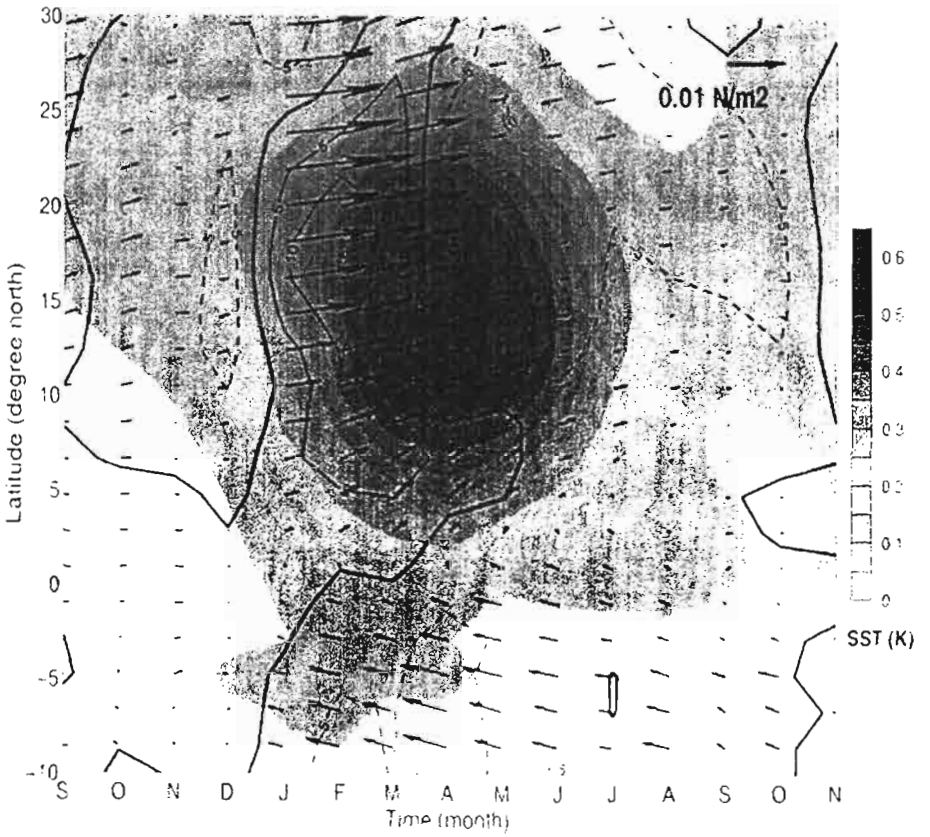

Figure 3.1: After CVM (their figure 2) : regressions onto the NTASST index, over 1950–1999 : anomalies of SST (color), net heat flux (contour, every $5W/m^2$), wind stress (vector). Data are from NCEP/NCAR.

According to CVM, one of the most striking event over the Tropical Atlantic is characterized by anomalous SST north of the equator, with modifications in the trade winds. To document the question, CVM have focused on the «NTA» region. They have defined the NTASST index as the mean of SST anomalies over this region, averaged from March to May (i.e. when most of the warming or cooling of the water occurs). The time serie obtained has 50 points (from 1950 to 1999).

They showed that almost every NTA event could be associated to one ENSO or one NAO (North Atlantic Oscillation) event. For instance, positive (negative) NTA events, i.e. with standard deviation larger (lower) than 1 (-1), are associated to 5 (8) El Niño (La Niña) events over 1950–1999.

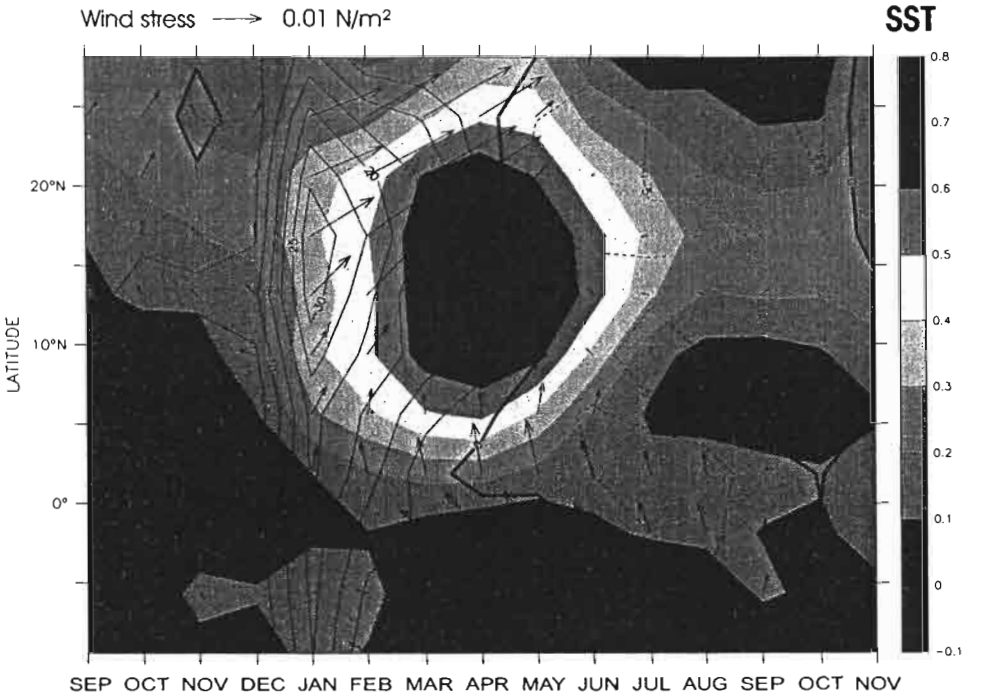

Figure 3.2: Same as figure 3.1, but for ECMWF data over the 1980–2000 period.

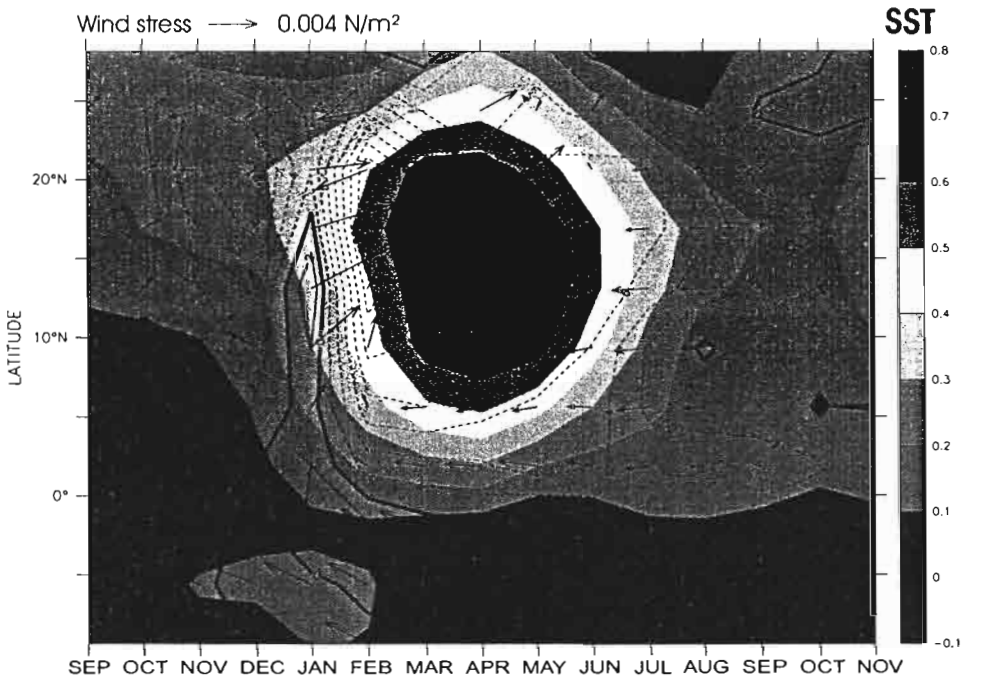

Figure 3.3: Same as figure 3.2, but for the QTCM outputs, over 1950-1999

3.1.1 Observations

CVM's results CVM's figure 2 is displayed as figure 3.1. In this figure, regressions of SST, wind stress and net heat flux anomalies (from NCEP/NCAR reanalysis) are done over the 1950–1999 period. Anomalies are zonally averaged between 40°W and 20°W, where the variability of NTASST peaks. For

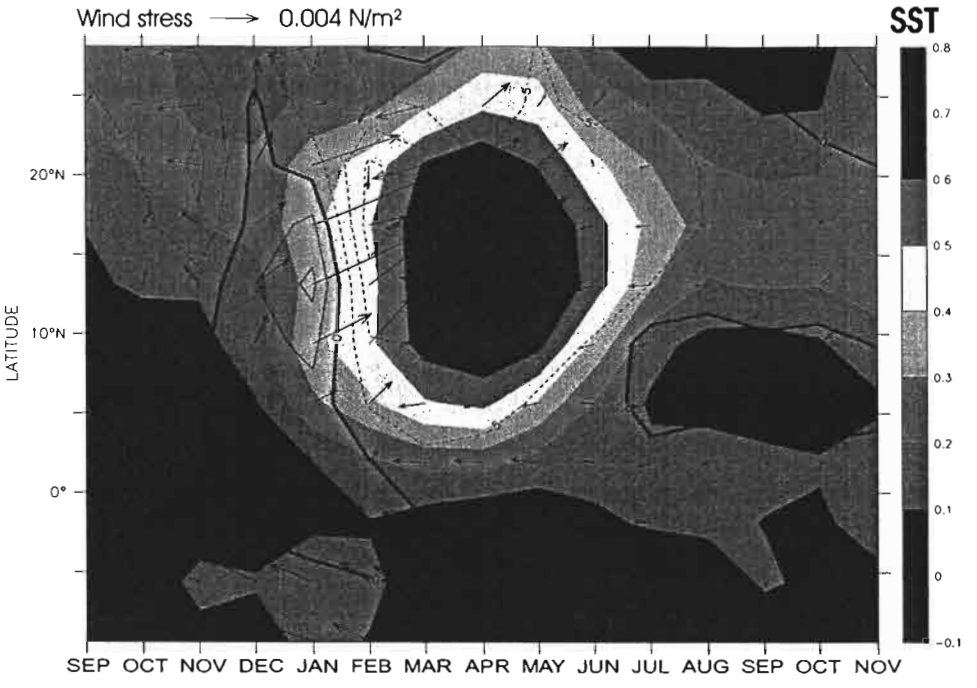

Figure 3.4: Same as figure 3.3, but over 1980–2000.

each field and each latitude, 15 time series (15 months, from September before March-April-May, to November after this period) are regressed onto the NTASST index. The derived slopes are multiplied by a standard deviation of 0.5 K.

A warming of the SST of about 0.5 K is found around March-April-May, between 5°N and 25°N. This is consistent with the definition of the NTASST index (see above). The warming is induced by a reduction in the trade winds from January to March. According to CVM, it leads to a reduction in the evaporation that induces positive net heat flux toward the ocean, of the order of 5 W/m^2 to 10 W/m^2, during the same period. These anomalies are responsible for the warming of the waters. After April, the trade winds anomalies disappear, and the SST anomalies decrease, through evaporations losses.

ECMWF data Figure 3.2 is similar to figure 3.1 but for ECMWF data. The comparison between the two maps is rather good if we focus on the region between 5°N and 25°N and between December and August. From January and during the winter, there is a weakening of the trade winds, before the warm SST anomalies. Simultaneously, the net heat flux toward the ocean is increasing, and keep positive until May. The wind anomalies are also comparable, both in location and in amplitude (0.01 to 0.02 N/m^2). From April, a cooling of the waters occurs, through evaporation feedback, like in CVM. However, there are noticeable differences, that may originate from the different data processings : we have used ECMWF data (1980-2000), while CVM used NCEP-NCAR reanalysis (Kalney and Coauthors [1996], Trenberth et al. [2001]), over a different time period (1950-99). We may note for example, that the ECMWF net heat flux anomalies (up to 30 W/m^2) are larger than in CVM (only up to 15 W/m^2). We may also remark that the ECMWF positive net heat flux anomalies last until April, while in the CVM study they only last until March. However the explanation of the mechanism leading to the SST anomalies proposed by CVM is in agreement with our results. Note that the amplitude of the negative net heat flux anomalies after May and north of 5°N are much lower than the amplitude of the positive anomalies that occur before May, suggesting that the decay of the warm SST anomalies is perhaps not controlled only by latent cooling, as it is suggested in CVM.

3.1.2 QTCM outputs

The figure 3.3 presents the results for the model outputs from the «CONTROL» run over the 1950–1999 period. Like in figure 3.1, a weakening of the trade winds and positive net heat flux anomalies are

found in winter. However, the positive anomalies of net heat flux are five to eight times less than those found by CVM. Moreover, they have very little extension in time and space : positive anomalies are found only in January north of 5°N at 2-3 W/m^2, which is not sufficient to explain the warm SST anomalies. This deficiency of the model also shows up in the winds, with anomalies that only last one month, when they last three to four months in the observations (figure 3.1). It is also not clear if a weakening in the trade winds leads to a reduction of the evaporation losses in QTCM.

Figure 3.4 is similar to figure 3.3, but for the 1980–2000 period. It tests the impact of the time period considered in the analysis. The positive net heat flux anomalies, and the weakening of the trade winds in winter extend more in time and space compared to figure 3.3. North of 5°N, they last two to three months instead of only one month in figure 3.3. However, net heat flux anomalies are still very weak, more than two times weaker than those of figure 3.2. Moreover, even if winds anomalies last longer, they are still a bit weak compared to the observations, as they never reach 0.02 N/m^2. In addition, the damping effects of heat flux on SST takes place much too early (February). Thus the SST anomalies still can not be explained by latent flux anomalies. Despite these discrepancies, in comparaison with figure 3.3, wind anomalies are better simulated over this period, both in amplitude and location. The inaccurate representation of the net heat flux may thus come from the ability of the model to simulate the evaporation weakening linked to a reduction of the wind speed. Sensitivity tests were carried in order to elucidate this point, and the results are presented in the appendix.

3.2 Regressions onto the NINO3 index

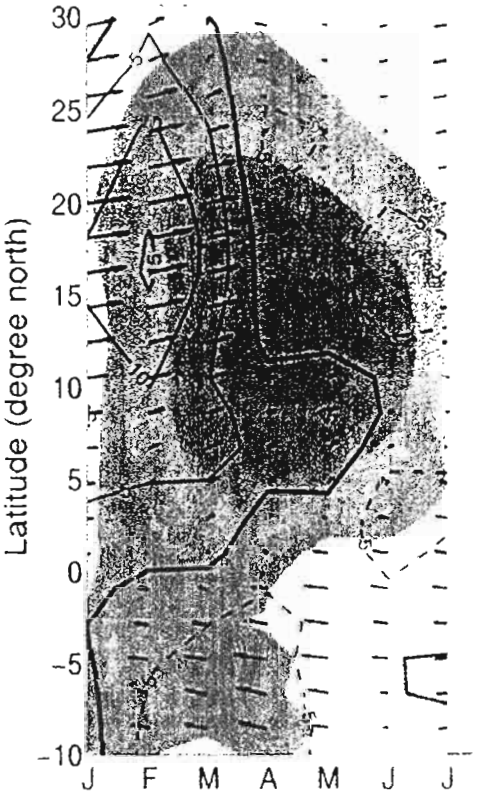

Figure 3.5: After CVM (their figure 5(a)). Same as figure 3.1 but regressions are done onto the NINO3 index.

CVM also carried out similar analysis than above, but regressing onto the NINO3 index, in order to estimate the role of remote forcing associated to ENSO. The NINO3 index is defined as the mean SST in the region 5°S-5°N / 90°W-150°W, averaged in winter (December-January-February). According to CVM, anomalous westerlies are associated with positive ENSO events, leading to reduced evaporation, and then to a warming of the water over the NTA region.

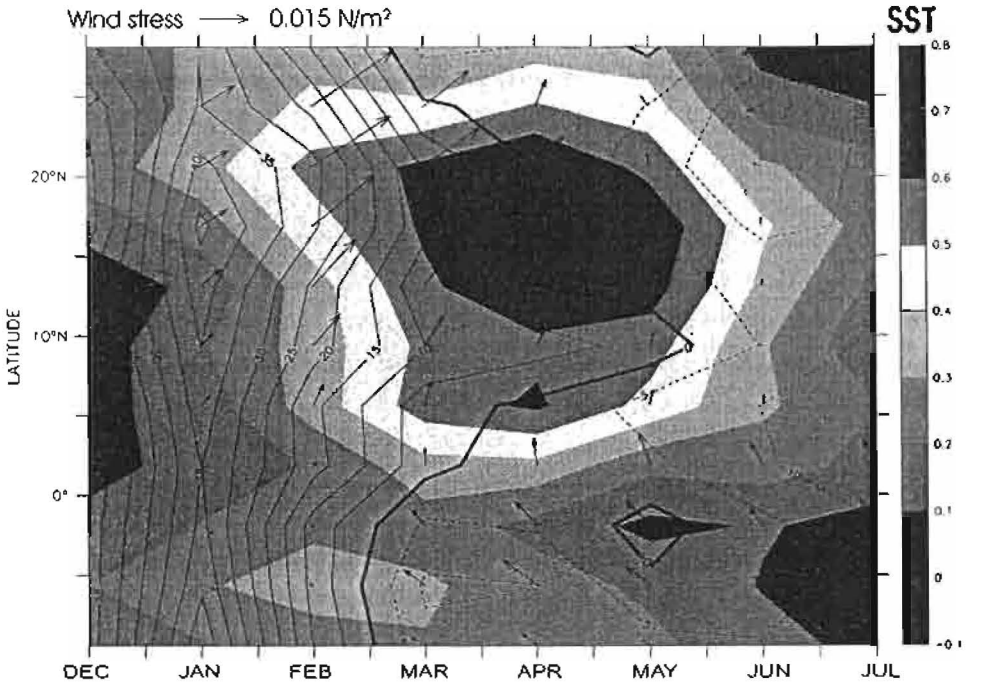

Figure 3.6: Same as figure 3.5, but for ECMWF data over 1980–2000.

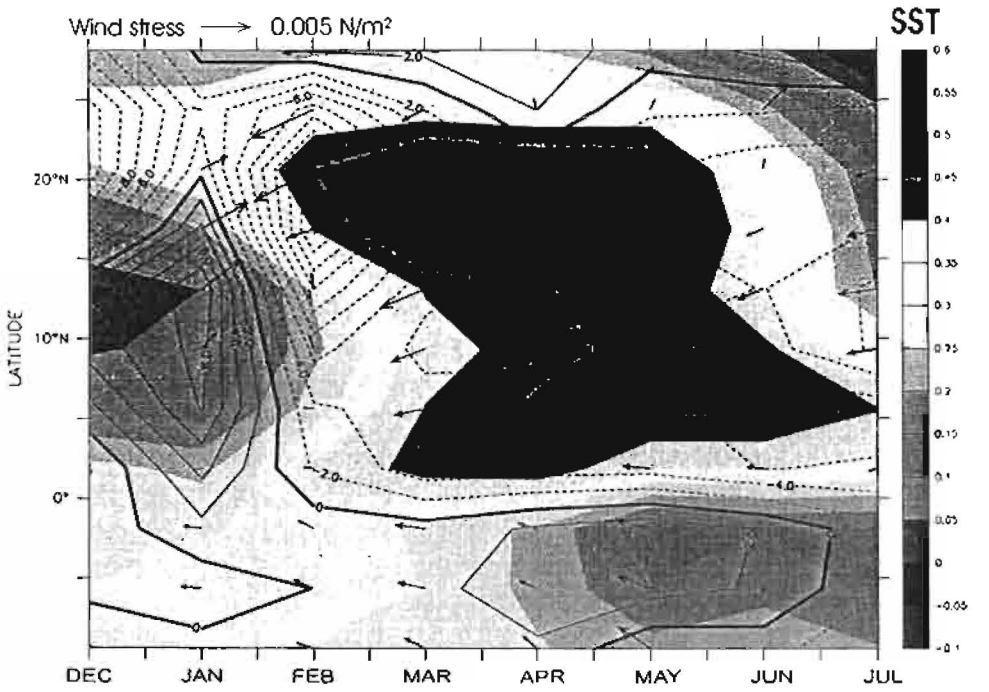

Figure 3.7: Same as figure 3.5, but for QTCM outputs («CONTROL» run) over the 1950–1999 period

3.2.1 Observations

CVM's results CVM's figure 5(a) is displayed in figure 3.5. SST, wind stress and net heat flux anomalies are regressed onto the NINO3 index, over the 1950–1999 period. A weakening of the trade winds is found, from January to March, associated with positive net heat flux anomalies through a

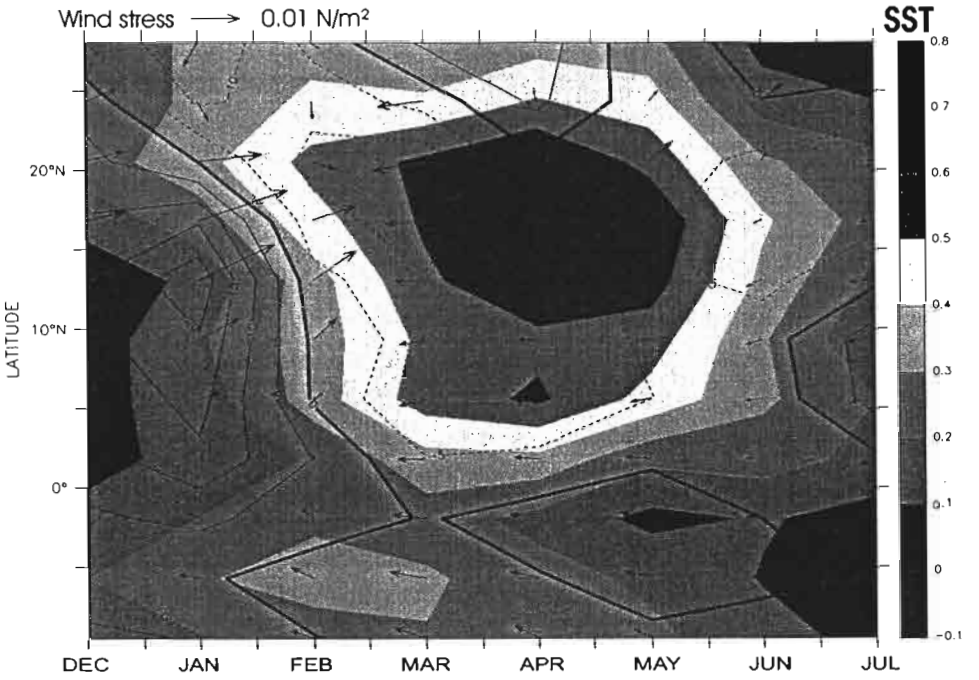

Figure 3.8: Same as figure 3.7 (QTCM outputs, «CONTROL» run) but over the 1980–2000 period

reduction of the evaporation losses. This induces the warming of the water found in MAM. Then the wind stress and net heat flux anomalies weaken, and a cooling of the waters occurs. Regressing onto the NINO3 index gives almost the same results than regressing onto the local NTASST index (cf. figure 3.1). According to CVM, this means that a remote forcing linked to ENSO plays a role in the SST variability in the NTA region. According to them, anomalous low pressures over the western subtropical gyre are partly responsible for the winds anomaly, and these anomalies are linked to the PNA (Pacific North American) pattern forced by ENSO events. Shifts in the Walker circulation during ENSO bring pressure anomalies in the tropics (cf. KSL), that also induce wind anomalies in the NTA.

ECMWF data Figure 3.6 is similar to figure 3.5, but for the ECMWF data. Positive net heat flux anomalies are induced by a weakening of the trade winds during the winter and until April, north of 5°N. They lead to a warming of the water in MAM. Then, when the net heat flux anomalies change sign, the SST anomalies start weakening. This is consistent with CVM. However, we can notice that the amplitude of the anomalies in net heat flux in figure 3.6 are larger than those found by CVM : up to 40 W/m^2 whereas they only reach 10 W/m^2 in CVM. The result indicates nevertheless that the mechanism of the forcing of SST anomalies in the NTA region by ENSO events proposed by CVM applies for the ECMWF data.

3.2.2 QTCM outputs

The figure 3.7 diplays the results for the model outputs over the 1950–1999 period. Positive net heat flux anomalies are found in December and January between 5°N and 15/20°N, like in the observations. However, the amplitude of these anomalies is lower than in CVM (less than 10 W/m^2), and they only last one or two months (DJ). This has to be related to the too weak (less than 0.01 N/m^2) and too brief trade wind anomalies. We find exactly the same discrepancies than in the results obtained from the regressions over the NTA index (cf. figure 3.3), confirming that the model with such forcing does not properly simulate wind stress and net heat flux anomalies associated to SST anomalies in the region.

For the 1980–2000 period (figure 3.8), similar differences than between figures 3.3 (QTCM, full period) and 3.4 (QTCM, 1980–2000) are found. The trade wind anomalies are in better agreement with those of figure 3.6, but the net heat flux positive anomalies north of 5°N are still too weak (two times less

than those of ECMWF data), and do not extend enough in time: they last less than three months, when the wind anomalies last three months, and the ECMWF flux positive anomalies last four to five months. The ability of the model to simulate evaporation anomalies induced by wind stress weakening is still in question with this map, as we see that in February there is no positive heat flux anomaly linked to wind stress reduction.

In order to further investigate the actual contribution of the Tropical Pacific, two model experiments were carried out, which results are presented below.

3.3 Experiments with regional interannual forcings

The SST variability in the NTA region is partly induced by remote forcing associated to ENSO. Local forcing could however also play a role in this variability. QTCM may thus improperly interpret one of these forcings, or, as will be seen, there are limitations to the use of forced simulations for the study of the processes under concern. Following Su et al. [2001], we have separated two different forcing regions. We have run QTCM over the 1950–2000 period using two modified SST fields.

- **«PAC» run** : in this run, anomalies over the 30°N-30°S / 100°E-80°W are kept, to isolate the SST forcing due to ENSO. Everywhere else, seasonal SST is used as boundary conditions.
- **«ATL» run** : in this run, anomalies over the 2°N-30°N / 80°E-10°W are kept, to isolate the forcing in the NTA region. Everywhere else, seasonal SST is used as boundary conditions.

Note that on every map, observed SST anomalies (without any mask) are used. Wind stress and net heat flux anomalies are QTCM outputs from the «ATL» and the «PAC» runs.

3.3.1 «PAC» run

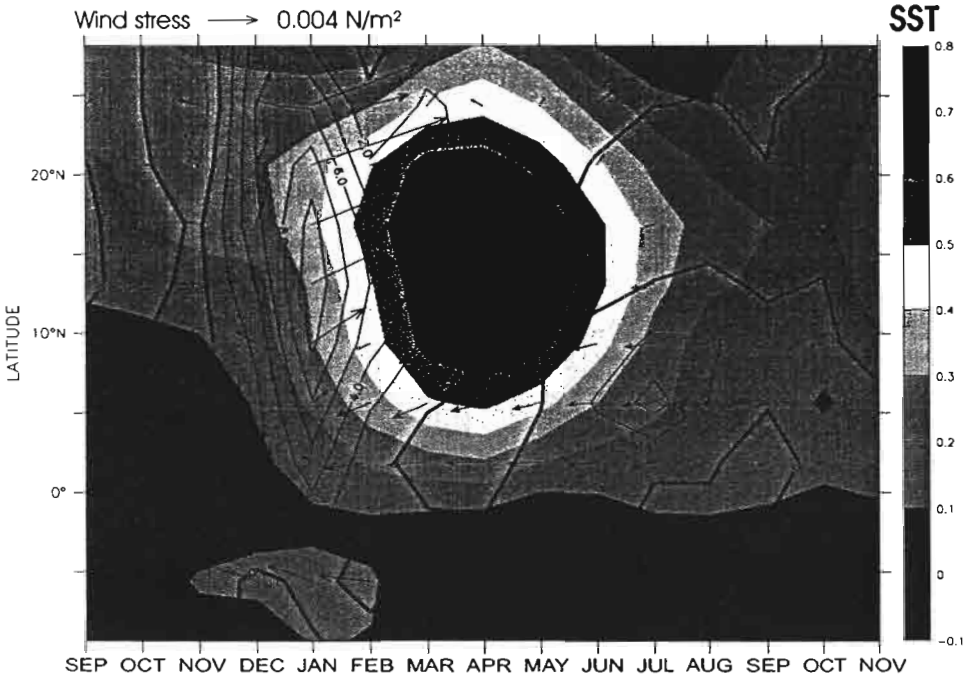

Figure 3.9: Same as figure 3.1, but for wind stress and net heat flux QTCM outputs from the «PAC» run.

Figure 3.9 is similar to figure 3.1, but for wind stress and net heat flux QTCM outputs from the «PAC» run. Negative (eastwards) wind anomalies are found in January and February north of 5°N, and to a lesser extent in December and March north of 15°N. They lead to positive net heat flux anomalies of the order of 8 W/m^2 from December to March, like in figure 3.1.

These anomalies last longer and extend more than in figure 3.3 («CONTROL» run), exhibiting a similar pattern than in the observations (figure 3.1). QTCM simulates thus a heat flux forcing associated to ENSO that contributes to SST increase in the NTA region. It is not seen with the «CONTROL» run.

Note that we get similar results if we do regressions on the NINO3 index or the ENSO index (results are displayed in the appendix).

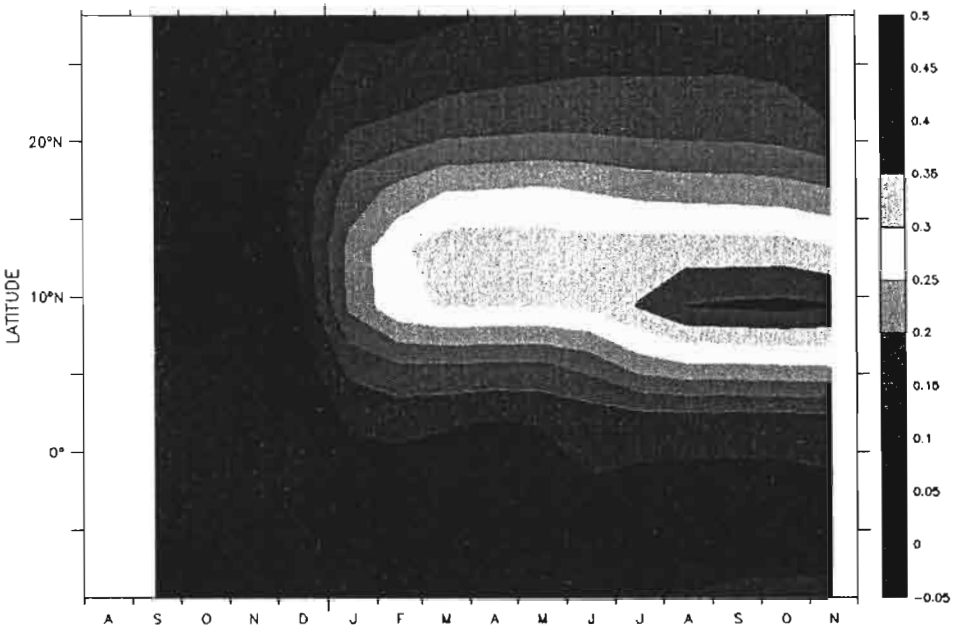

Figure 3.10: Temperature anomalies obtained from the flux computed with the «PAC» run: $T = \int_0^t \frac{Q_{net}}{\rho C_p \overline{H}_{mix}} dt'$.

An estimation of the SST anomalies associated to the spatio-temporal heat flux structure can be estimated assuming no contribution of advection and dissipation, and seasonal variations in the mixed layer depth. It is given by :

$$T = \int_0^t \frac{Q_{net}}{\rho C_p \overline{H}_{mix}} dt' + T(t=0)$$

where:

- ρ is the density of the water, $\rho = 10^3\ Kgm^{-3}$,
- C_p is the calorific capacity of water $C_p = 4.18\ J/g$,
- $\overline{H}_{mix}$ is the monthly mixed layer depth derived from the TAOSTA data (Vauclair and du Penhoat [2001]) over 1979-1999,
- Q_{net} the net heat flux entering the ocean.

Note that tests have been made (not shown) that show that there is not much difference if climatological or real time mixed layer depth is chosen. $\frac{Q_{net}}{\rho C_p \overline{H}_{mix}}$ has been regressed onto the NTASST index (like the net heat flux anomalies in section 3.1), and integrated as a function of time from the month of September (t=0). We observe a warming from January between 5°N and 20°N, that peaks to 0.35 K in March-April-May around 10°N. This is about 50% of the warming found in the observations. It means that, without local air-sea interaction, ENSO should be responsible for about 50% of the NTA variability. Past April, in this run there is no cooling of the waters associated to negative heat flux anomalies. This cooling is likely to be due to local forcing.

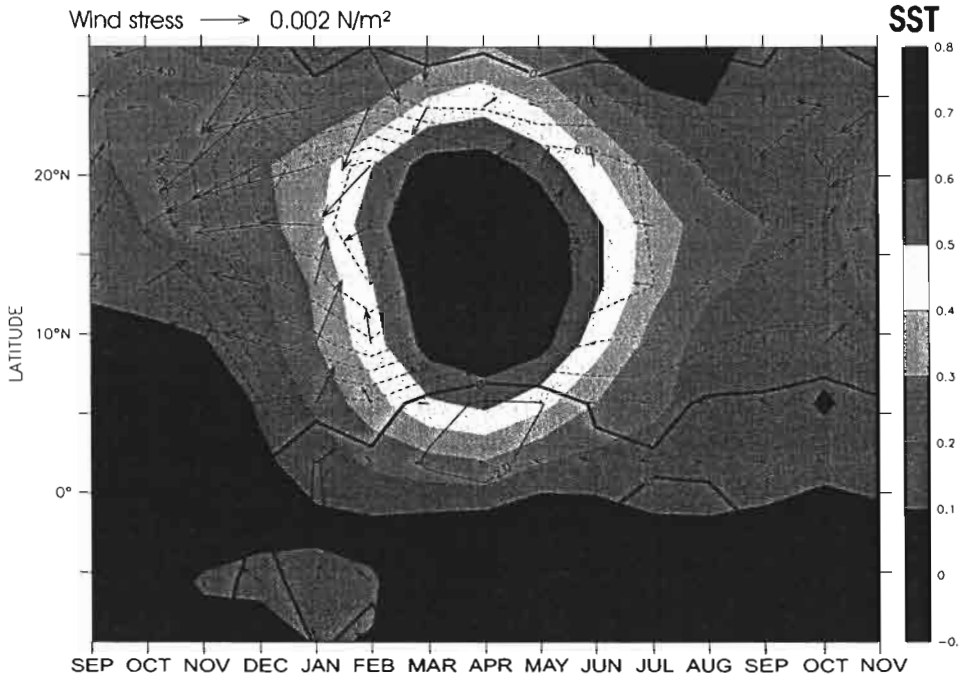

Figure 3.11: Same as figure 3.1, but for wind stress and net heat flux QTCM outputs from the «ATL» run.

3.3.2 «ATL» run

The «ATL» run should provide an estimate of the local forcing contribution, or at least the way the QTCM model will respond to these local SST anomalies.

Figure 3.11 is similar to figure 3.9, but for the QTCM outputs from the «ATL» run. The local forcing in the NTA region opposes the ENSO forcing. The «ATL» forcing tends to strengthen the trade winds, (while the ENSO forcing tends to weaken them). The largest wind stress westwards anomalies (of the order of 0.002 N/m^2) are found from November to February north of 10°N. They begin earlier than the eastwards wind stress anomalies from the «PAC» run (November vs December-January), and they have a weaker amplitude (0.004 N/m^2 vs -0.008 N/m^2 in January). These anomalies lead to negative net heat flux anomalies which are centered in February north of 10°N, and of the order of -10 W/m^2 (vs +8 W/m^2 in the «PAC» run). These negative net heat flux anomalies are also more widely spread in space and time compared to those forced by ENSO (see figure 3.9). It may explain the results from the «CONTROL» run, where almost no positive net heat flux are found.

We find negative net heat flux anomalies after April, i.e. after the warming of the waters. This indicates that heat losses operate through evaporation associated to warm SST. However, it is not clear why large anomalies eastwards winds and negative net heat flux anomalies are found before March. Easterlies of the order of 0.005 N/m^2, prior to January are indeed found around 20°N, associated to negative net heat flux anomalies of the order of 10 W/m^2. We should not find anomalous evaporation losses before the warming of the water. This may be due to the absence of remote SST anomalies in the Pacific that modify the convection cells in the Tropical Atlantic. However, these anomalies probably exists in the «CONTROL» run and are opposing the anomalies induced by the Pacific forcing. They are responsible for the too weak eastwards wind stress anomalies and positive net heat flux anomalies from December to March.

Note that similar results are obtained with regressions onto the NINO3 index and the ENSO index, confirming our analysis (displayed in the appendix).

The results suggest that superposing the two runs leads to a similar situation to the «control» run.

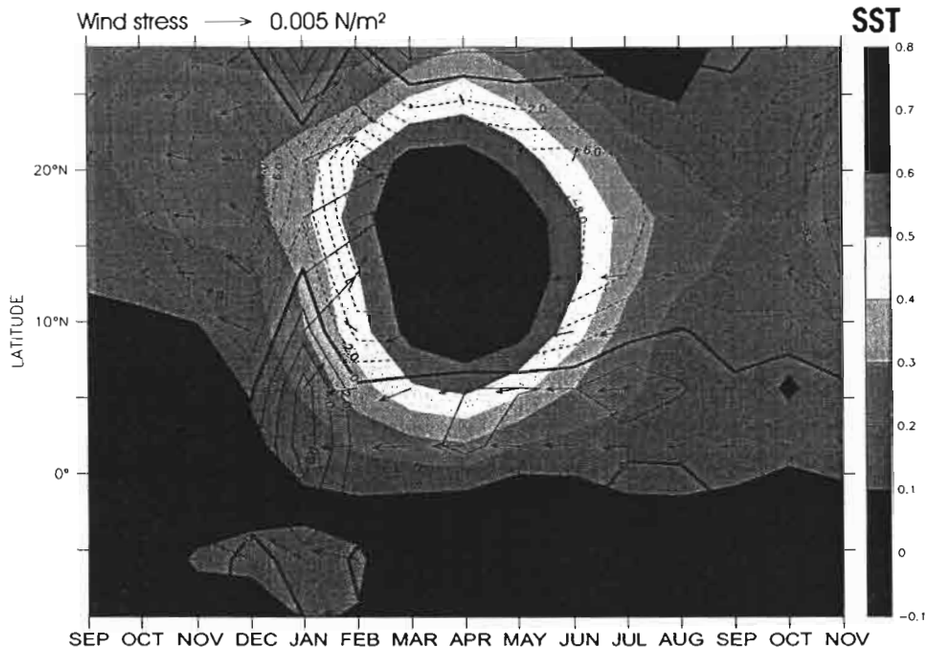

Figure 3.12: Superposition of wind stress and heat flux anomalies from figure 3.9 («PAC» run) and figure 3.11 («ATL» run).

3.3.3 Superposition of the two runs

We have superposed the wind and flux anomalies from figure 3.9 («PAC» run) and figure 3.11 («ATL» run). This has to be compared to figure 3.3 («CONTROL» run). North of 10°N, negative net heat flux anomalies have almost the same amplitude and location, and are of the same order (-7 W/m^2 around November and -11 W/m^2 around March). We find similar results for the wind stress anomalies. We find a noticeable difference between December and February for net heat flux anomalies, suggesting this is the time period when non-linearities in the model have the largest amplitude. In the «CONTROL» run (figure 3.3), positive net heat flux anomalies are found in January north of 15°N. In the superposition, the positive net heat flux anomalies in January are only located below 15°N. For example, at 15°N in January, the heat flux anomalies due to non-linearities are of the order of 4 W/m^2. This is likely to be the location and time period when the coupling between the ocean and the atmosphere may be the more unstable.

Doing the regressions onto the NINO3 and the ENSO index, we find similar results (displayed in the appendix).

Apart from the contribution of non linearities, it may be possible to find a combination between the forcings that would reproduce more accurately the variability in the NTA region. The forcing linked to ENSO may be underestimated, so it could be possible to strengthen it, through some parameters adjustments (see appendix for sensitivity tests). Or the local forcing may be overestimated, and there may be a way to weaken its influence. Nevertheless, it is not clear where these improper estimations could come from.

Conclusion

We have used the QTCM model (version 2.3 released in August 2002) and observations to investigate the ENSO teleconnections over the Tropical Atlantic. In particular, we have tested the ability of QTCM to simulate teleconnections in the Northern Tropical Atlantic, where most of the SSTA variability is found. The QTCM model was designed to simulate the tropical variability. It is quite successful to reproduce the low frequency variability in the equatorial band (Neelin and Zeng [2000], Zeng et al. [2000]). However its ability to simulate the variability at latitudes of 15-20°N was not assessed thoroughly.

Our study shows evidences that the model has some skills in reproducing the SST, heat flux and wind relationship in the NTA region. In particular, our work shows that the warming of the waters in the NTA region is strongly correlated to the ENSO forcing. On the contrary, the cooling of the waters is locally controlled. However, the local SST forcing is probably overestimated and/or the remote forcing associated to ENSO is underestimated.

Despite these discrepancies, we have to keep in mind that QTCM is used in a forced context, which prevent us to draw firm conclusions. The use of a coupled model is needed. Accounting that remote forcings play a large role in the SST variability in this region, all the issues linked to that kind of use of the model may be amplified in the NTA region

At this stage, several points are raised :

- The land model has maybe a major role in the spreading of the ENSO effects from the Pacific to the Atlantic. In particular, sensitivity experiments are needed to understand the effect of the Cordilleras, which is simply modeled through friction at the surface.
- Approximations in the model that have been chosen to simplify the equations are well adapted to describe large scale convective phenomenons. They lead to good results in the Pacific equatorial band, but the NTA region is not so wide and further from the equator. The approximations may thus fail to describe the variability in such a region. In particular the local forcing may be affected, and overestimated. For example, the evaporation heat losses due to the the warming of the water may be too high.
- Prescribing observed SST as boundary conditions is probably responsible for a large part of the discrepancies found between simulations and observations, because the heat flux equilibrium at the ocean surface is not set up. It seems necessary to use a couple model to further investigate the issue of ENSO teleconnections over the NTA region.

APPENDIX

The appendices present the results of sensitivity tests and experiments done with QTCM.

- **Appendix** A : KSL have also investigated the influence of ENSO in remote regions. We reproduce some of their work done on wind stress and net heat flux variability in the Tropical Atlantic.
- **Appendix** B : we present the resutlts of the regressions onto the NINO3 and the ENSO index, obtained from the two specific forcings used in section 3.3.
- **Appendix** C : parameters are changed in QTCM and we evaluate their influence. Some aspects of the land model, the boundary mixed layer, and the evaporation-wind feedback are tested. The evaporation–wind feedback parameterization is also used to reduce the intraseasonal variability in the «ATL».
- **Appendix** D : we compute correlations and significance tests for regressions maps done in our study.

From this additionnal work, some more conclusions can be drawn. Some points are still in question.

- It is confirmed that the role of the local forcing is preponderant in QTCM. QTCM responds above all to the NTA forcing (appendix B). In particular, flux during the decrease of an SST event are very correlated to the local SST (appendix D). The forcing coming from the Pacific is most of time hidden by the local response (appendix B).
- Non-linearities are found in QTCM in the NTA region. They are located in january around 15°N and 35°W (appendix B).
- Removing a part of the intraseasonal variability in QTCM in changing the parameterization of the evaporation weaken the inluence of local forcing in QTCM (appendix C.4).
- Forcing the model and not coupling it to an ocean model is probably part of the source of the QTCM discrepancies in the NTA region.

A Regressions onto the ENSO index

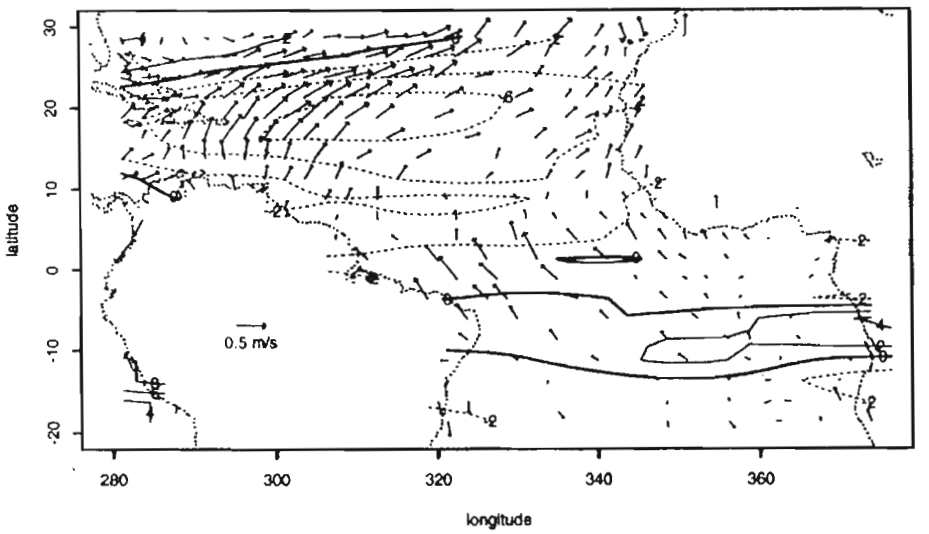

Figure A.1: After KSL (their figure 8(a)). Regressions of surface wind (vector), and latent heat flux (contour, W/m^2) anomalies onto the ENSO index, over the 1950–1999 period, for the months of JFMA. Observations are from EECRA.

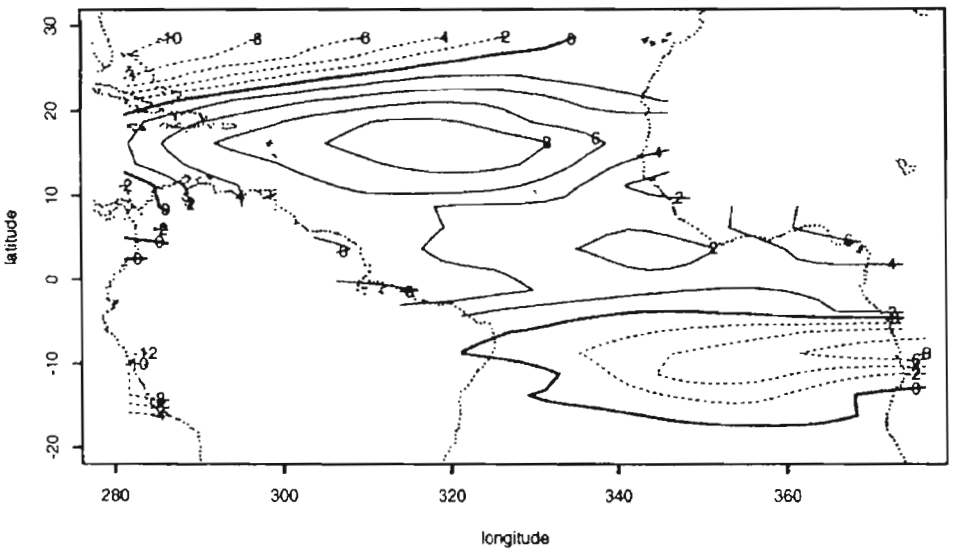

Figure A.2: After KSL (their figure 8(c)). Regressions of net heat flux onto the ENSO index (W/m^2), over the 1952–1992 period, for the months of JFMA.

KSL have also investigated the question of El Niño teleconnections in the NTA region, and proposed the same mechanism than CVM. They have used the ENSO index. Contrary to CVM, they do not average this index over any time period. However, to focus on the ENSO variability, a 3 months running mean is done on this index. According to KSL, changes in evaporation are very correlated to the ENSO index and control the net heat flux anomalies. The latters due to wind anomalies partly induced by modifications in the convective cells over the NTA region during ENSO events.

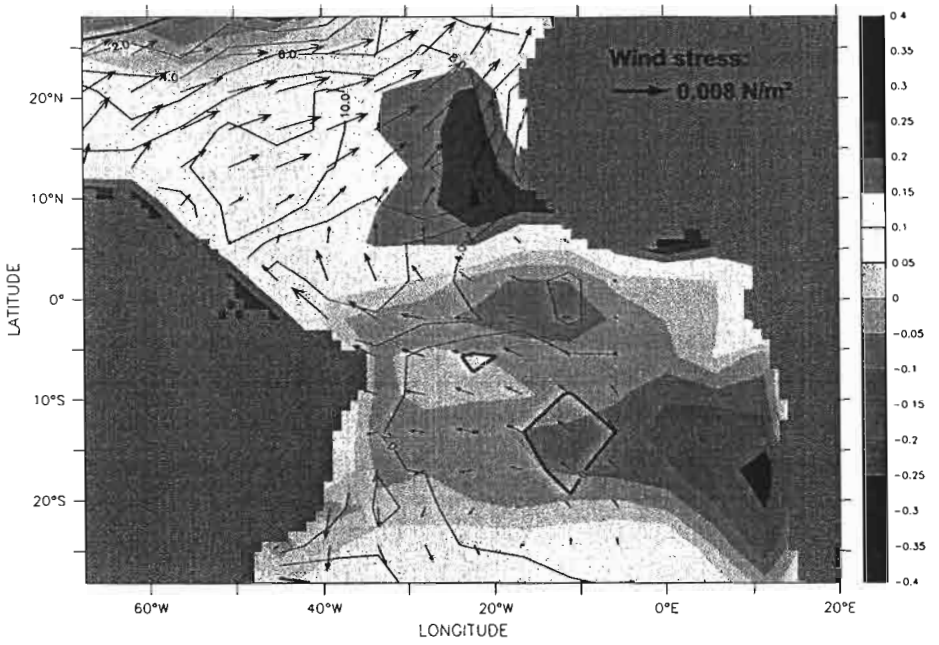

Figure A.3: Same regressions as figures A.1 and A.2, but for SST (color), wind stress (vector), and net heat flux (contour, W/m^2) anomalies, for ECMWF data over the 1980–2000 period.

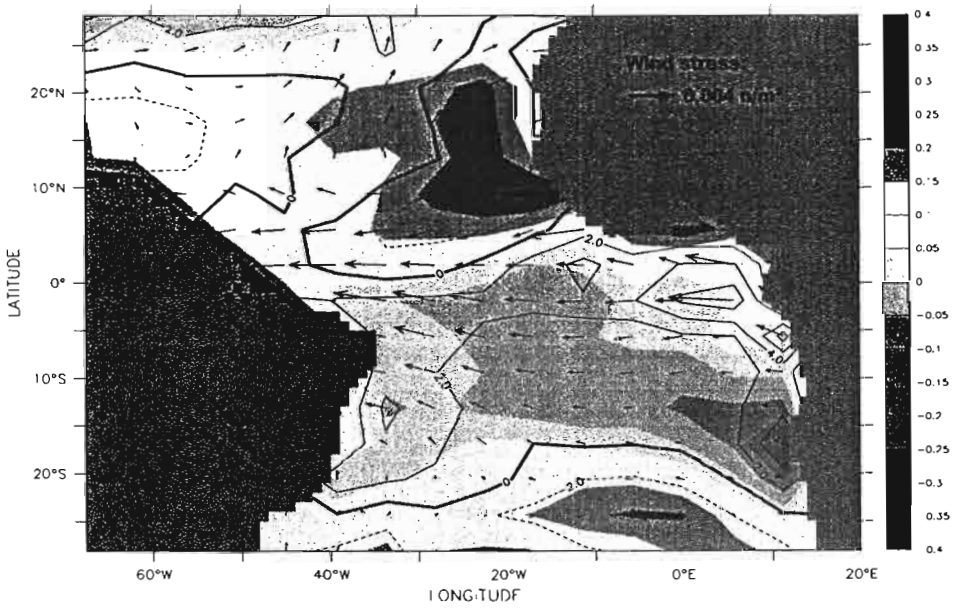

Figure A.4: Same as figure A.3, but for QTCM outputs, over the 1952–1992 period.

A.1 Observations

KSL's results KSL's figure 8(a) and 8(c) are displayed in figure A.1 and figure A.2. KSL have use a compilation of ship reports, in an extended version of the Edited Cloud Report Archive (ECRA, Hahn et al. [1996], see KSL for details on Extended ECRA). Surface wind, latent heat flux and net heat flux

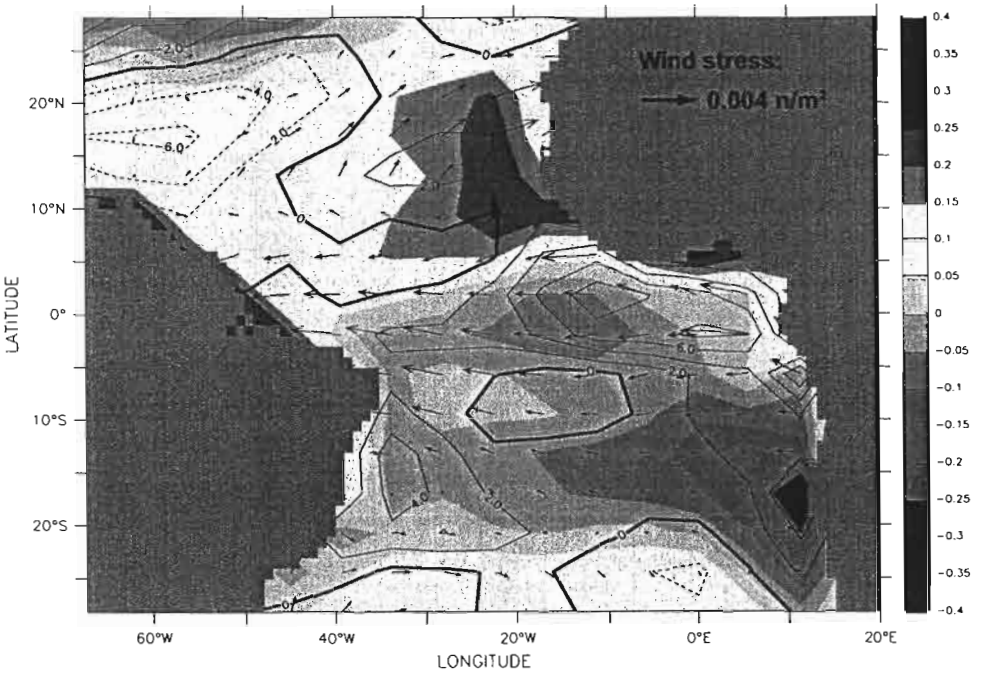

Figure A.5: Same as figure A.4, but for the 1980–2000 period (QTCM outputs).

anomalies are regressed onto the ENSO index, over the 1952–1992 period. The anomalies of January, February, March and April (JFMA) are regressed onto the January, February, March and April values of the ENSO index. Then the mean of the derived four slopes values is taken, and multplied by the standard deviation of the ENSO index.

Positive net heat flux anomalies of the order of 6 to 8 W/m^2 are found between 10°N and 20°N and between 60°W and 20°W (figure A.2). They are associated with westerlies that are due to ENSO, according to KSL (figure A.1), and reduction in the evaporation losses. This is in agreement with the mechanism proposed by CVM. Note that the variability is weaker in the equatorial band, and that negative anomalies are found between 5°S and 15°S. We can also remark that positive (resp negative) net heat flux anomalies (figure A.2) are associated with negative (resp positive) latent heat flux anomalies (figure A.1). This shows evidence that heat flux anomalies during an NTA event are controlled by latent anomalies.

ECMWF data Figure A.3 is similar to figure A.2, but using ECMWF data, over the 1980–2000 period. We also display SST anomalies (Reynolds and Smith [1994]), and wind stress anomalies (ECMWF data). We observe positive net heat flux anomalies over the entire NTA region, in agreement with KSL. The anomalies have similar amplitude in this area than in KSL (between 6 and 10 W/m^2). In the south of the Tropical Atlantic, anomalies are negative in KSL, but not in our analysis (only near zero). The warm SST anomalies are located north of 5°N, in agreement with CVM. Observing the wind stress anomalies, the mechanism leading to SST anomalies and already discussed, is confirmed again. An observed weakening of about 0.005 N/m^2 in wind stress causes a reduction in the evaporation losses, leading to positive net heat flux anomalies of the order of 8 W/m^2.

A.2 QTCM outputs

Figure A.4 is similar to figure A.3, but for the QTCM outputs, over the 1952–1992 period. The net heat flux variability is quite low in the equatorial band, like in KSL (of the order of 2 W/m^2). Wind stress anomalies in the equatorial band are also realistic : westerlies of the order of 0.004 N/m^2 are found, which is lower than in figure A.3, but may depend on the time period used for the calculation. Easterlies are also found north of 15°N like in the observations. However, they are about three times lower, and they

do not lead to positive net heat flux anomalies. It gives another evidence of the difficulties for QTCM to link realistically wind stress anomalies with latent heat flux anomalies in this region.

Figure A.5 is similar to figure A.4, but for the 1980–2000 period. North of 5°N, we observe a weakening of the trade winds, and positive net heat flux anomalies, west of 40°W. Similarly than in figures 3.4 and 3.8, wind stress and net heat flux anomalies are better simulated over the 1980-2000 period than over the 1950–1999 period. Concerning wind stress, a good agreement is found between QTCM and observations over a large part of the Tropical Atlantic, west of 40°W, and in the equatorial band. The latent heating anomalies are however less than 4 W/m^2 over the region where warm SST anomalies occur, instead of 8 W/m^2 like in the observations.

A.3 Conclusion

This analysis confirms the results found in sections 3.1 and 3.2. A good agreement is found between QTCM and the observations in the equatorial band. Rather good results are also found in the NTA region for the wind stress anomalies, in better agreement with the observations than those found in the studies inspired by the work of CVM. However, these anomalies are too weak. Moreover, they are not associated with net heat flux anomalies. It may illustrate the difficulties for QTCM to associate wind stress anomalies and latent heat flux anomalies. It may also mean that, in QTCM, latent heat flux variability is not controlled enough by wind stress anomalies, but probably more by SST anomalies. To further investigate this issue, sensitivity experiments were performed (displayed in Appendix C). It remains however difficult to conclude on this from the results of these experiments.

B Additional analyses from the «PAC» and «ATL» runs

Regressions onto the NINO3 and the ENSO indexes have been performed for runs «PAC» and «ATL».

B.1 «PAC» run

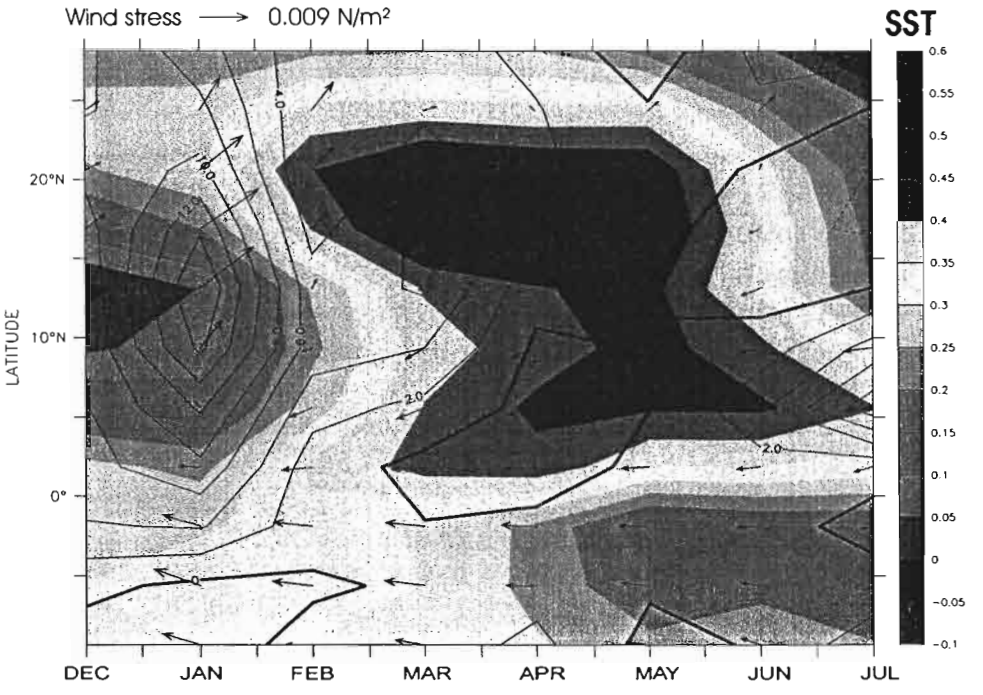

Figure B.1: Same as figure 3.5 (regressions onto the NINO3 index), but for wind stress and net heat flux QTCM outputs from the «PAC» run.

Figure B.1 is similar to figure 3.5, but for «PAC». Positive net heat flux anomalies are found from December to April, confirming that ENSO plays a role in the warming of SST in the NTA region. The negative heat flux anomalies that should be associated to the cooling of the waters after April do not appear, suggesting that they are due to the local SST anomalies (not prescribed in this run).

Figure B.2 is similar to figure A.2, but for «PAC». Positive net heat flux anomalies are found over the NTA region, west of 40°W, associated to wind stress weakening. Even if these anomalies are very weak (of the order of 2 W/m^2, versus 6 W/m^2 in KSL), it provides another evidence of the the ability of QTCM to simulate ENSO teleconnections over the NTA region.

B.2 «ATL» run

Figure B.3 (resp figure B.4) is simiar to figure B.1 (resp figure B.2), but for «ATL».

Like in figure 3.11, we find a strengthening of the trade winds before and after the warm SST event, that leads to negative net heat flux anomalies over the NTA region. After May, these anomalies are due to the positive SST anomalies.

However, negative net heat flux anomalies and easterlies prior to January are also found, even when the waters are not anormaly warm yet. It is still not clear why such anomalies are found. The absence of SST anomalies in the Pacific may not only lead to the absence of weakening of the trade winds, but could also create anomalous easterlies in the Atlantic.

B.3 Superpostion

Wind stress and net heat flux of figure B.1 («PAC» run) and B.3 («ATL» run) are superposed in figure B.5. This maps is comparable to figure 3.7 («CONTROL» run), indicating that in QTCM,

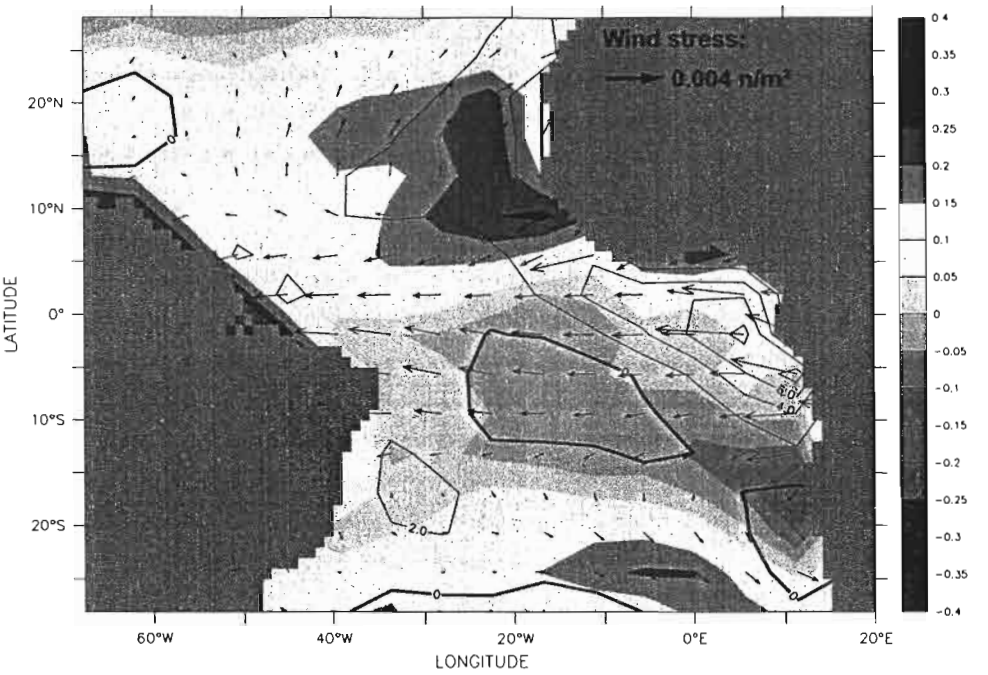

Figure B.2: Same as figure A.2 (regressions onto the ENSO index), but for wind stress and net heat flux QTCM outputs from the «PAC» run.

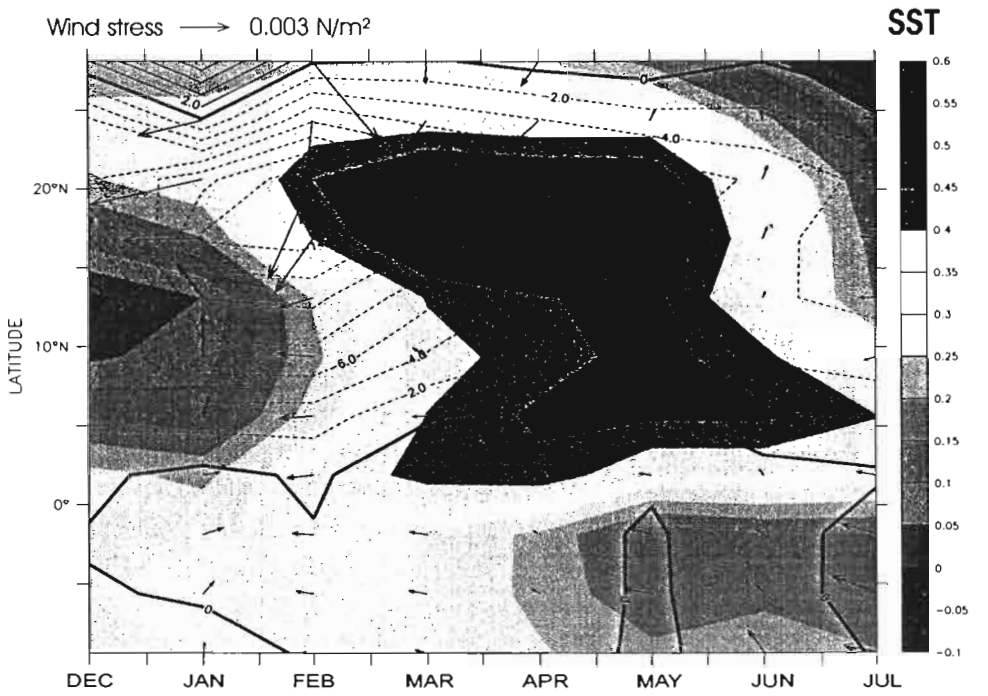

Figure B.3: Same as figure B.1 (regressions onto the NINO3 index), but for wind stress and net heat flux QTCM outputs from the «ATL» run.

the combination of local and remote forcing in the NTA region is almost linear. Nevertheless, as in figure 3.12, a noticeable difference with the «CONTROL» run is found in january between 15°N and 20°N. In figure 3.7 («CONTROL» run), positive net heat flux anomalies of the order of 4 W/m^2 are found in this area. In figure B.5, they are of the order of 0 or -2 W/m^2. It suggets that at this time

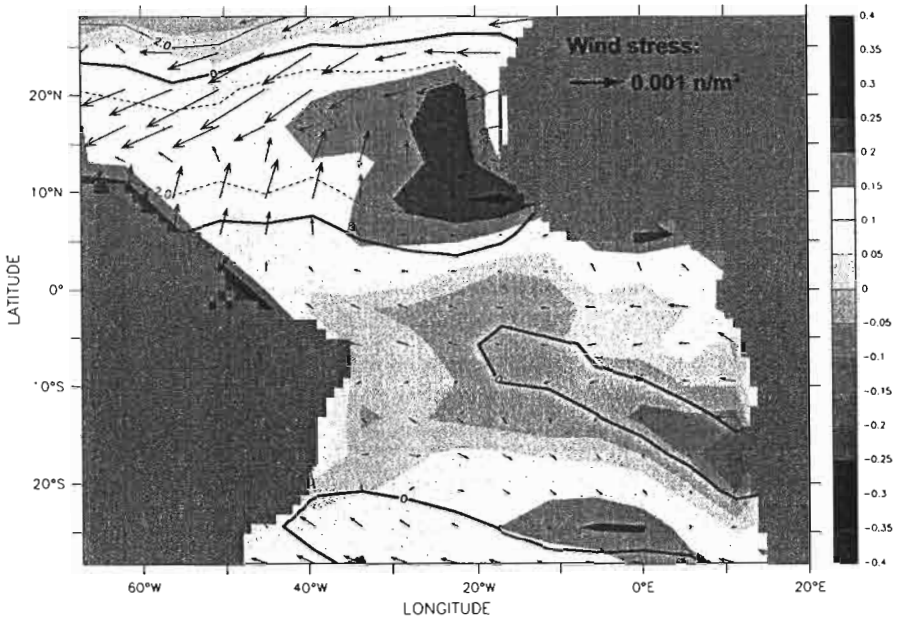

Figure B.4: Same as figure B.2 (regressions onto the ENSO index), but for wind stress and net heat flux QTCM outputs from the «ATL» run.

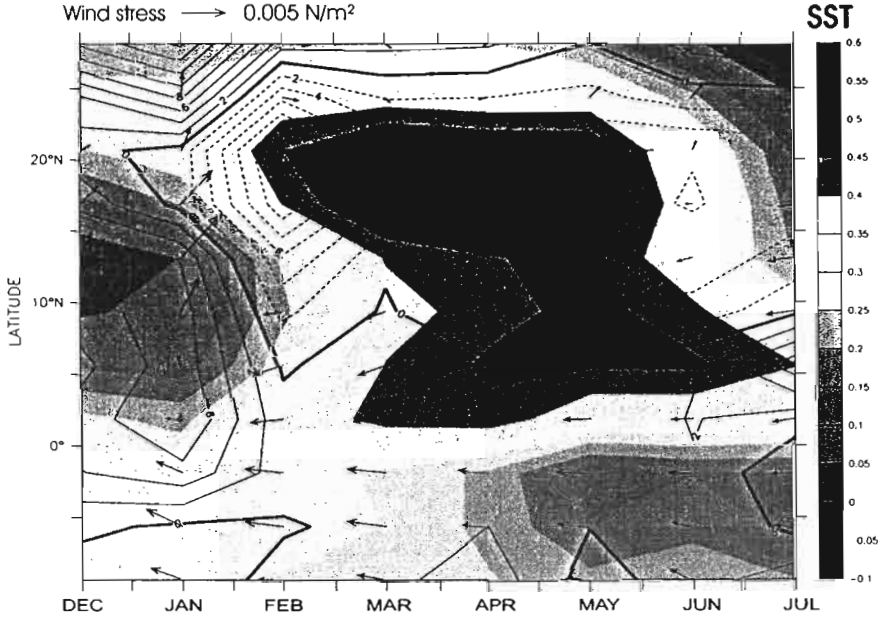

Figure B.5: Superposition of wind stress and heat flux anomalies from figure B.1 («PAC» run) and figure B.3 («ATL» run).

period and at this location, a coupling between ocean and atmosphere is likely to take place. The net heat flux anomalies due to these non-lincarities are of the order of 5 W/m^2.

Similarly wind stress and net heat flux of figure B.2 and B.4 are superposed in figure B.6.

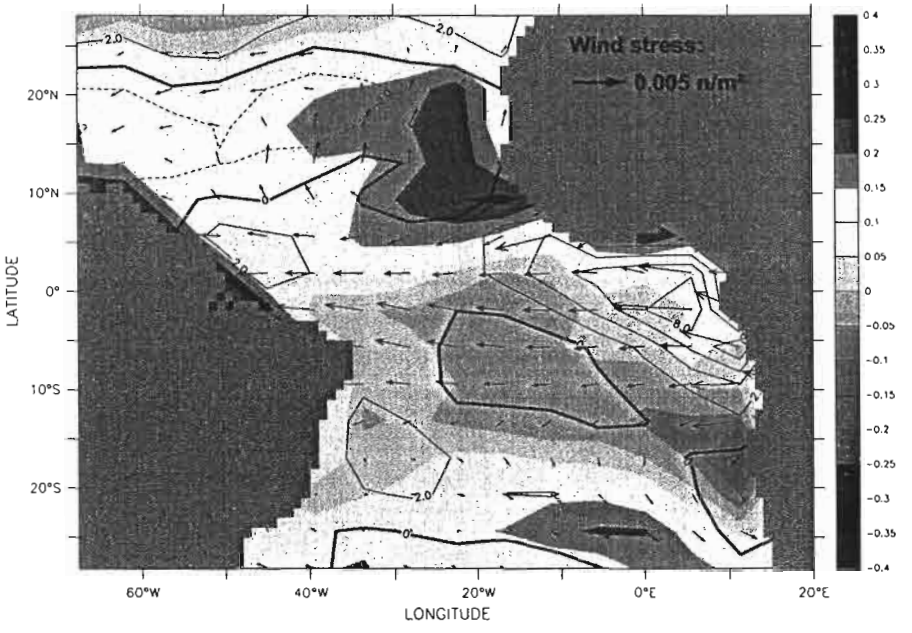

Figure B.6: Superposition of wind stress and heat flux anomalies from figure B.2 («PAC» run) and figure B.4 («ATL» run).

The same non linearities are found if we compare this map and figure A.4. In the «CONTROL» run, positive net heat flux anomalies are found between 10°N and 20°N, and between 40°W and 30°W, instead of the negative anomalies found in figure B.6. The anomalies due to non-linearities in the «CONTROL» run are of the order of 3 W/m^2.

B.4 Conclusion

This part confirms the results obtained in section 3.3. First, a forcing in the NTA region associated to ENSO is simulated by QTCM. It should be responsible for positive (during an El Niño event) net heat flux anomalies in the NTA region, leading to the warming of the waters. However, this forcing is probably underestimated, and the local SST tends to conteract it between December and March. This is all the most surprising that this local forcing during the winter is likely to be due to warm SST that does not exist at this time period. Nevertheless, the local forcing also control the end of the warm event, through enhanced evaporation losses.

Finally, the combination between the two forcing is almost linear. However, some non-linearities are found in january, aroud 15°N and 35°W, that lead to net heat flux anomalies of the order of 4 W/m^2 in the «CONTROL» run.

C Sensitivity tests

C.1 Description of the runs

We have made three new runs in addition to those presented above. Our goal is to test the sensitivity of the model to different parameters that have influence upon wind stress and/or net heat flux.

- **«reduced intraseasonal variability» run**:

  QTCM simulates a reasonably broadband tropical intraseasonal variability (cf. Lin et al. [2000] for QTCM version 2.1). The source of this intraseasonal variability is shown to come from the effects of evaporation-wind feedback and excitation by midlatitude storms. In QTCM, it is possible to switch off these two sources : it consists in specifying a mean ($V_s(x,y)$) (the surface wind speed), and a mean horizontal advection of anomalous temperature (advT1 notation from the QTCM manual guide). Those mean fields are obtained by running the model forced with climatological SST and taking the mean over three years (cf. Lin et al. [2000]).

- **«landoff» run** :

  In this run we have cut off the land model. The temperatures over continents are thus «fake» temperatures. The convective cells may thus be altered. Consequently this will have an influence on both the net heat flux and the wind stress anomalies.

- **«NO_ABL» run** :

  We have used the «NO_ABL» option in this run (see QTCM manual guide). The surface flux are estimated without atmospheric boundary layer. It will test the impact of taking into account the boundary layer, which was not present in earlier versions of the model.

C.2 Correlations between QTCM and ECMWF

C.2.1 Wind stress

Correlations between QTCM and ECMWF for TAUX anomalies were calculated, for every run described above, in the Tropical Atlantic, over the 1980–2000 period (figure C.1). The variability is rather realistic around the equator, whatever the run, with correlations around 0.5 between 40°W and 20°. Almost everywhere else, we find correlations below 0.2, like for the «control» run. The results indicate that there is little impact of parameters changes on TAUX anomalies. Note however that the Boundary Layer model tends to improve the correlations between simulation and observations in the Central Tropical Atlantic (+0.1 between 30°W and 20°W compared to the «control» run). We note also a slight improvement for the «reduced intraseasonal variability» run (in comparison with the «control» run), where we get correlations greater than 0.3 in the NTA region.

C.2.2 Net Heat Flux

Correlations between QTCM and ECMWF for net heat flux anomalies were calculated, for every run described in the previous part, in the Tropical Atlantic, over the 1980–2000 period (figure C.2). On each map, we can see rather strong correlations (greater than 0.3) around the equator, confirming that better results are found in the equatorial band with QTCM. Note however that these are more on the east (25°W-5°W) than the strong wind stress correlations (45°W-20°W).

However, net heat flux correlations are not as strong as wind stress correlations (0.3-0.4 versus 0.5-0.6). Moreover, the rather strong wind stress correlations found between 5°N and 20°N and between 20°W and 10°W are not associated with high net heat flux correlations. Very low, or even negative correlations are found in this region in every other run, instead of the 0.2-0.3 correlations found in the «control» run. This indicates that wind stress and evaporation anomalies are not properly linked. Net heat flux anomalies may also be due to radiative or sensible heat flux anomalies, and not only to latent heat flux anomalie, but some tests made (not shown) prove that the net heat flux variability in the Tropical Atlantic is mainly due to evaporation variablity in QTCM.

The parameters changes do not have much influence on net heat flux. Note however that cutting off the land model improvre the correlations with observations in the equatorial band around 10°W. However it was not seen for TAUX anomalies. TAUY anomalies may be more realistic in this area with no land model or sensible or radiative heat flux may be modified with this parameter.

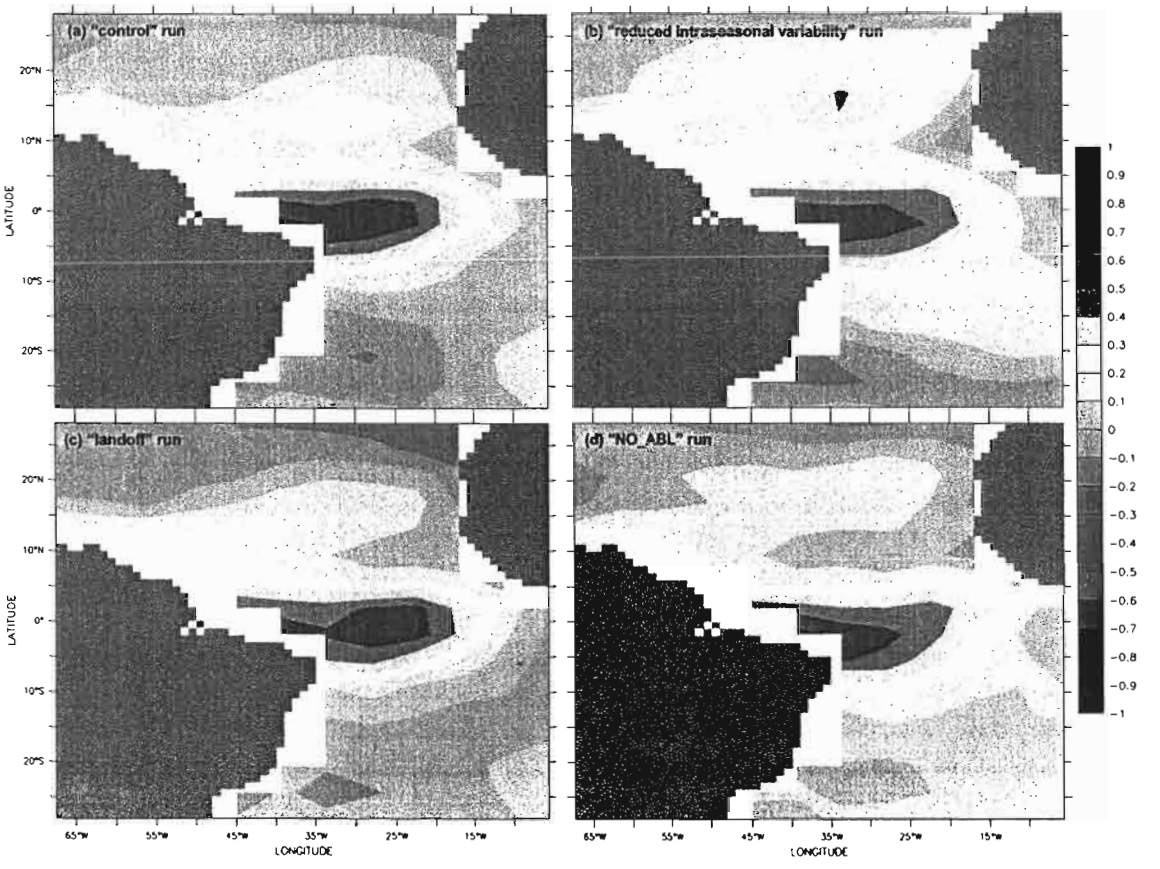

Figure C.1: Correlations between QTCM TAUX output and ECMWF TAUX data, over the 1980–2000 period, for each test of sensitivity.

C.3 QTCM variability

C.3.1 Wind stress

We have drawn RMS (Root mean square) maps to see where is located the wind stress variability, both with ECMWF data (fig. C.3) and QTCM outputs (fig. C.4). We can see from observations (fig. C.3) that the major part of the wind stress variability in the tropical Atlantic is located north of 10°N, with variability greater than 0.02 N/m^2, and to a lesser extent south of 10°S (more than 0.014 N/m^2). Around the equator and along the north western coast of Africa, there is almost no wind stress variability (less than 0.010 N/m^2).

If we consider the QTCM outputs, the variability in the equatorial band is lower than anywhere else, like in the observations. In the «control» run, the «landoff» run and the «NO_ABL» run, most of the varibility is located north of 10°N and south of 10°S, like in the observations. However, whatever the run, and whatever the area, the variability is much than in observations (about two times lower). It is not surprising that a model such as QTCM does not reproduce all the variability, because of the simplifications in the equations, or of the resolution for example.

The «control» run is the run that reproduces the best the observations. Removing the boudary mixed layer affects the variability, as it was seen in the correlations map presented above. It is also not surprising to find almost no variability in the «reduced intraseasonal variability» run (under 0.008 N/m^2).

C.3.2 Net heat flux

The same maps have been drawn for net heat fluxes in figure C.5 and C.6.

We can see from the observations (fig. C.5) that the net heat flux variability in the Tropical Atlantic

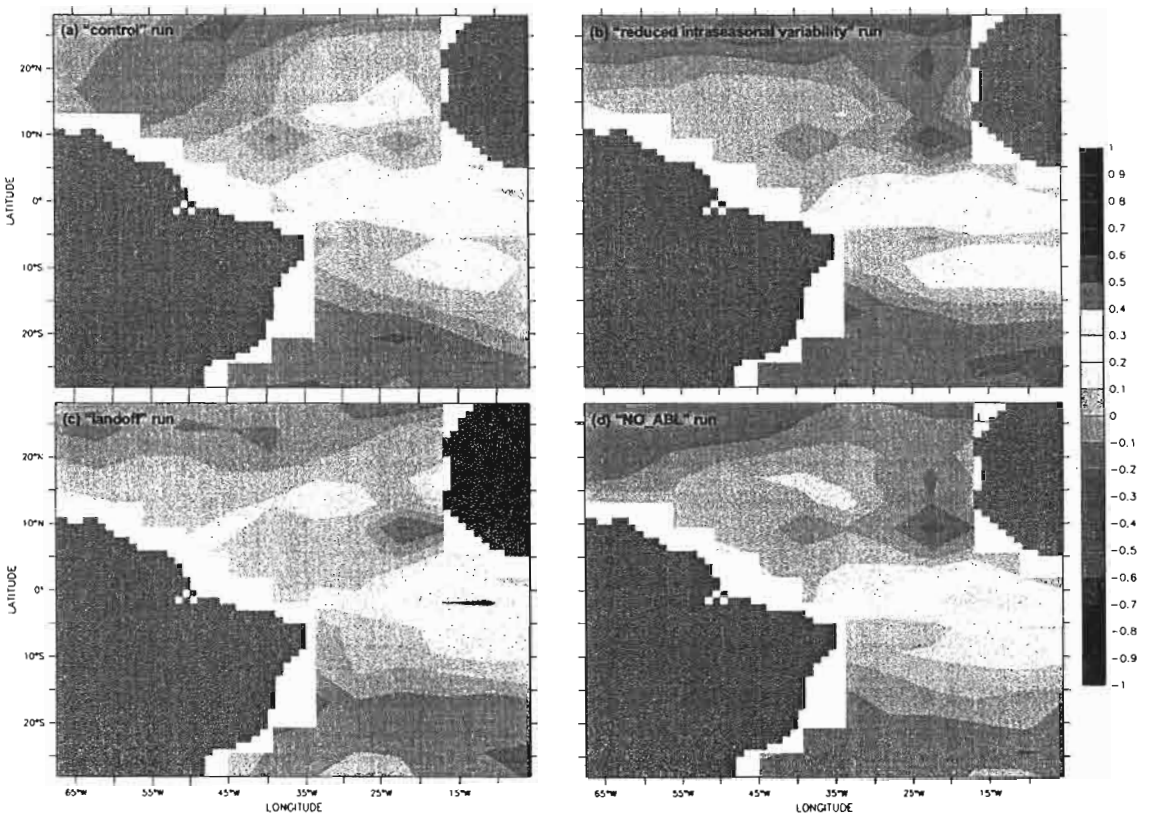

Figure C.2: Correlations between the anomalies of QTCM net heat flux output and ECMWF net heat flux anomalies data, over the 1980–2000 period, for each test of sensitivity.

is rather homogeneous (around 30 W/m^2). Note a slight exception east of 25°W between 10°N and 10°S, where the variability is below 20 W/m^2. Another exeption is found along the bresilian coast south of 20°W where the variability peaks to 45 W/m^2

Like for wind stress, the net heat flux variability in QTCM is 1.5 to 2 times lesser than in the observations. Except in the «landoff» run, the low variability found in the observations on the east of the basin is found, but not the high variability near Brasil. Like for wind stress, switching off the land model increases the net heat flux variability in the Topical Atlantic. On the contrary, the variability in the «reduced intraseasonal variability» run has decreased, in comparison with the «control» run (less than 10 W/m^2 over the NTA region for example). We have ued this parameterization to reduce the influence of the local forcing in the NTA region.

C.4 Reducing the intraseasonal variability in the «ATL» run

The local forcing in the NTA region may be overestimated. It may be linked to a too large intraseasonal variability. Following Lin et al. [2000], we have run a new «ATL» run using the same parameterization as in the «reduced intraseasonal variability» run, described in C.1.

Like in section 3.3, we have done regressions of SST, net heat flux, and wind stress anomalies onto the NTASST index, over the 1950–1999, for the outputs of this new «ATL» run. We have superposed the results obtained with those of the «PAC» run, like in figure 3.12.

As expected, the influence of the local forcing is weakened compared to the first «ATL» run. In this new experiment, the weakening of the trade winds begins from December instead of January like in the previous experiment superposing the two runs. They are also larger (0.004 N/m^2 vs less than 0.002 N/m^2) in February, and still exist in March. These anomalies are associated to positive net heat flux anomalies, that last from December to February and that extend as far a 20°N (instead of 10-15°N).

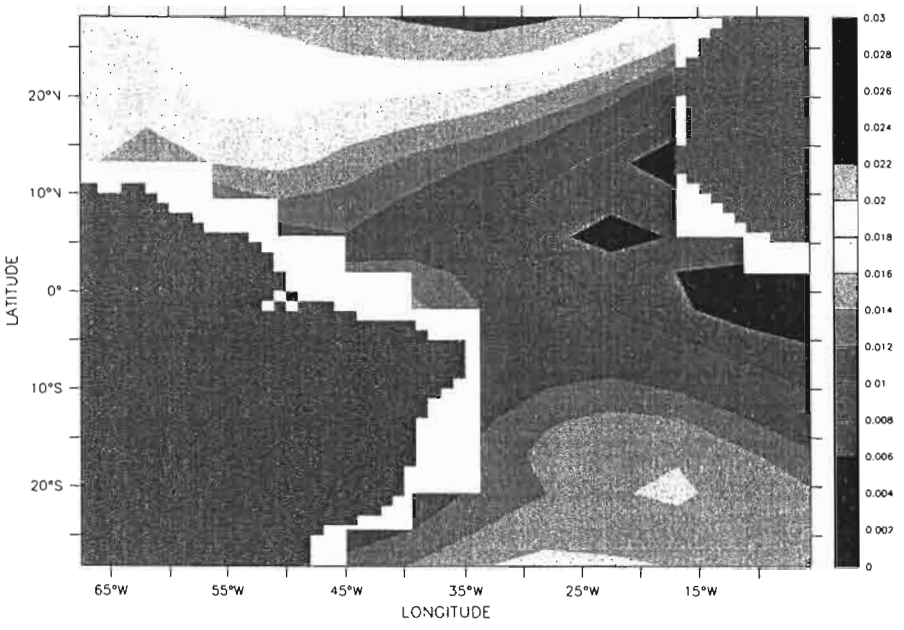

Figure C.3: wind stress RMS (N/m^2), ECMWF observations

This run is in better agreement with observations than the «CONTROL» run (figure 3.3). Reducing the influence of the local forcing by removing the contribution induced by intraseasonal variability gives thus better results. However, the net heat flux obtained still do not last enough and are not widespread enough compared to the observations.

C.5 Conclusion

The changes made in the parameterization of QTCM do not have much influence on wind stress and net heat flux variability in the Tropical Atlantic. However, the «control» run is the most realistic run. Better results are found using the atmospheric boundary layer. This is an improvement of the last QTCM version compared to the earlier, in which this layer was not present. We also note that removing the land model increases the QTCM variability, but does not improve the correlations with the observations. Finally, the parameterization used in the «reduced intraseasonal variability» run cuts off a large part of the variability in the NTA region.

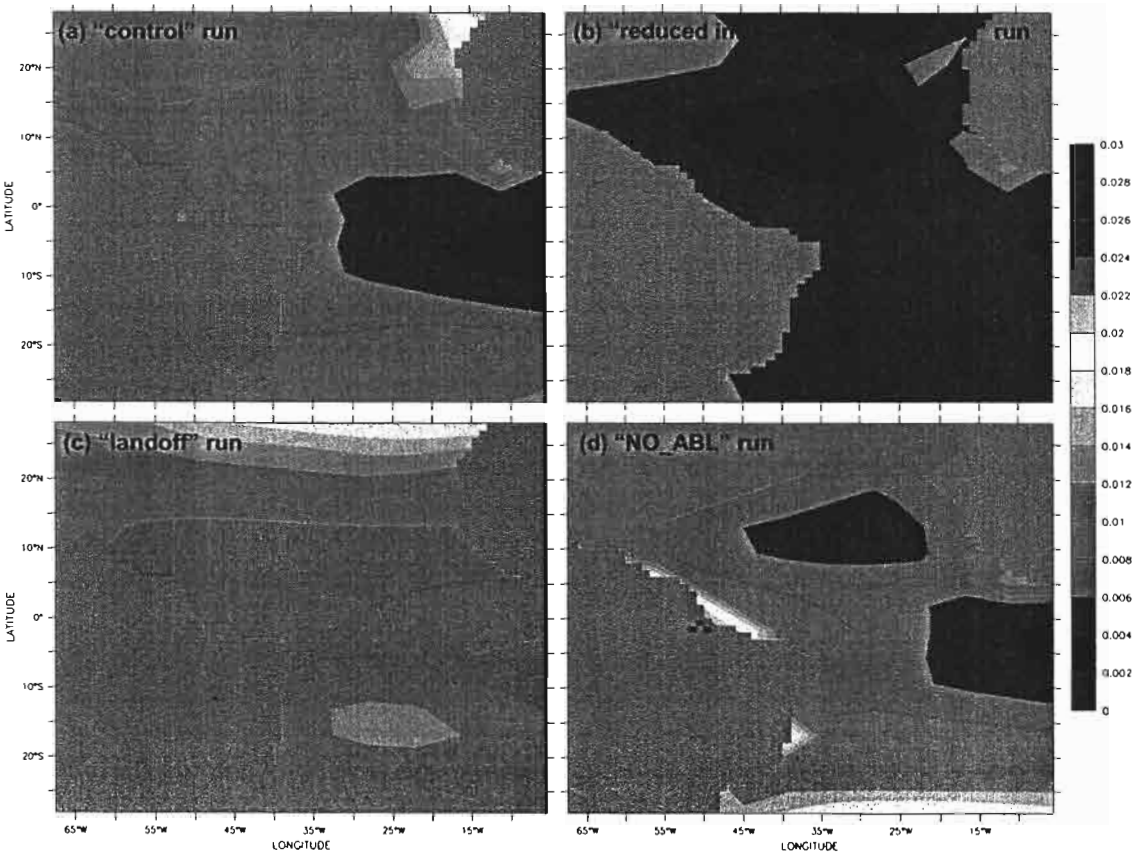

Figure C.4: wind stress RMS (N/m^2), QTCM outputs

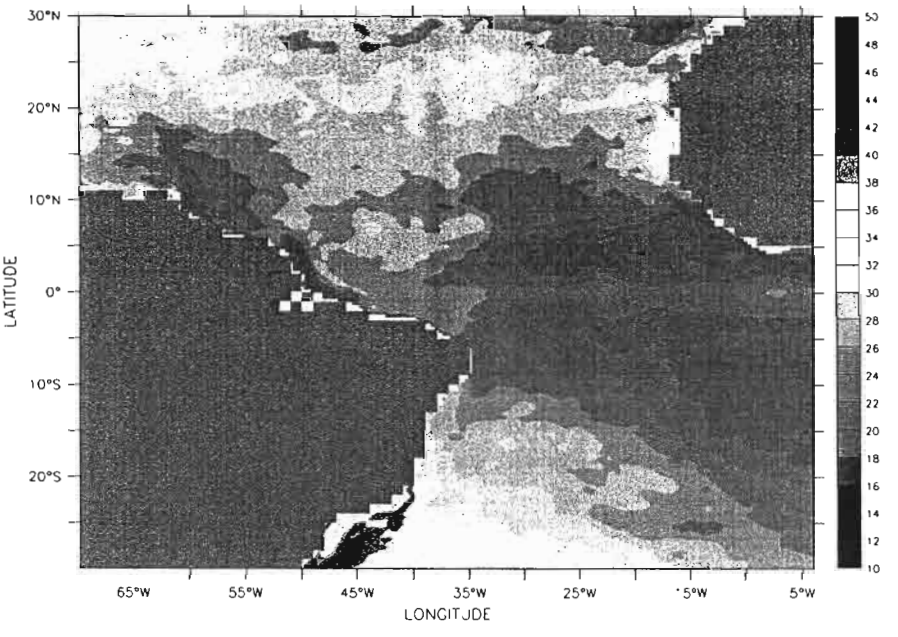

Figure C.5: net heat flux RMS (W/m^2), ECMWF observations

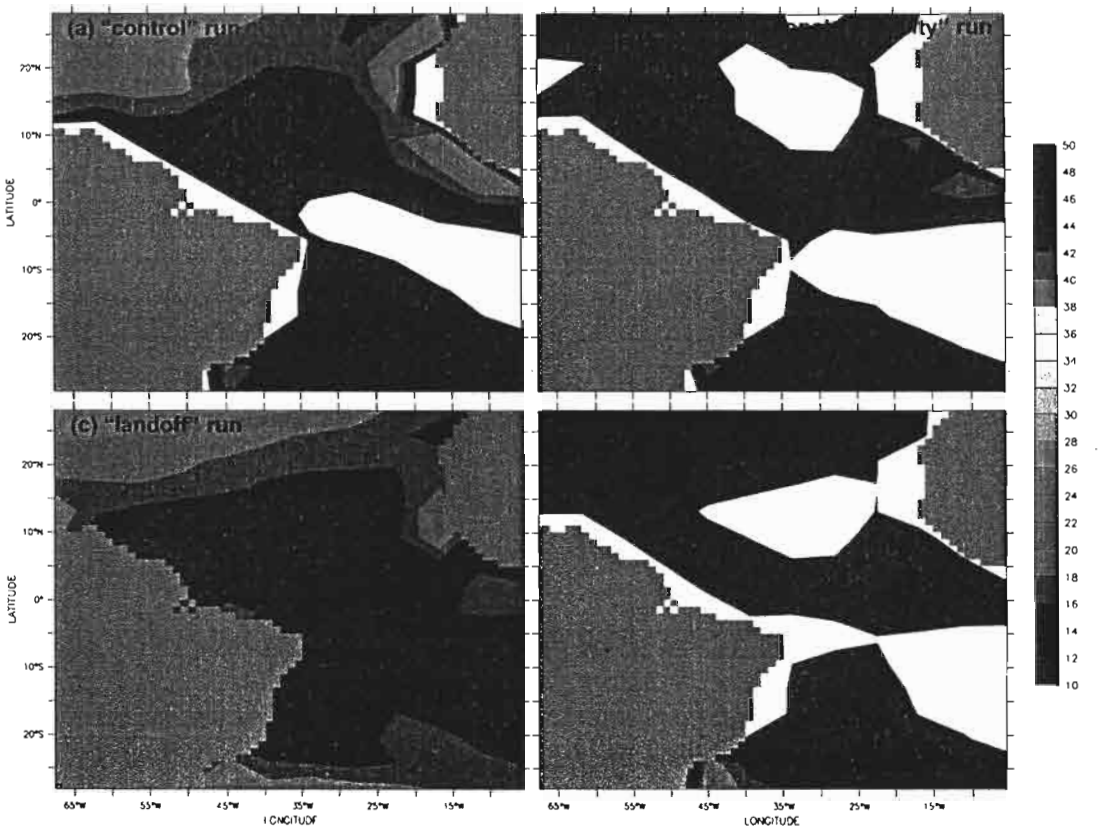

Figure C.6: Net heat flux RMS (W/m^2, white if under 10 W/m^2), QTCM outputs

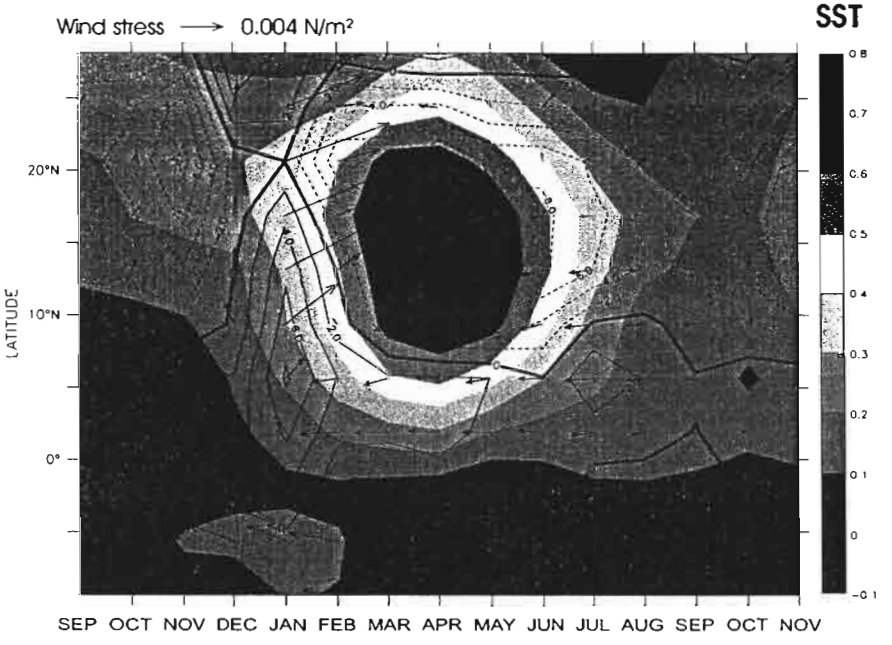

Figure C.7: Same as figure 3.11, but for the «ATL evaporation-wind feedback» run.

D Correlations and significance tests

D.1 Theory

We have computed correlations from these regressions and test their significance. Each time we have regressed an anomaly field Y (SST, net heat flux, wind stress), onto an SST index X (NTASST, NINO3, ENSO). We have calculated the «a» giving $Y = aX + b$. We can also compute α giving $X = \alpha Y + \beta$. Pearson's r^2 correlation coefficient is given by $r^2 = a\alpha$. The more r^2 is close to 1, the more X and Y should be correlated. The significance level of a correlation can be estimated, using the «t table» of Student. If N is the length of the time series, and r the Person's correlation coefficient,

$$t = |r| \frac{\sqrt{N-2}}{\sqrt{1-r^2}}.$$

t must be greater than a value given by the «t table» if we want the correlation to be significant at a certain level.

In our study, this minimum value of r^2 depends on the time period used. Choosing the significance at a 95% level, we get :

- r^2 greater than 0.19 for the 1980–2000 time period,
- r^2 greater than 0.08 for the 1950–99 time period.

D.2 Correlations

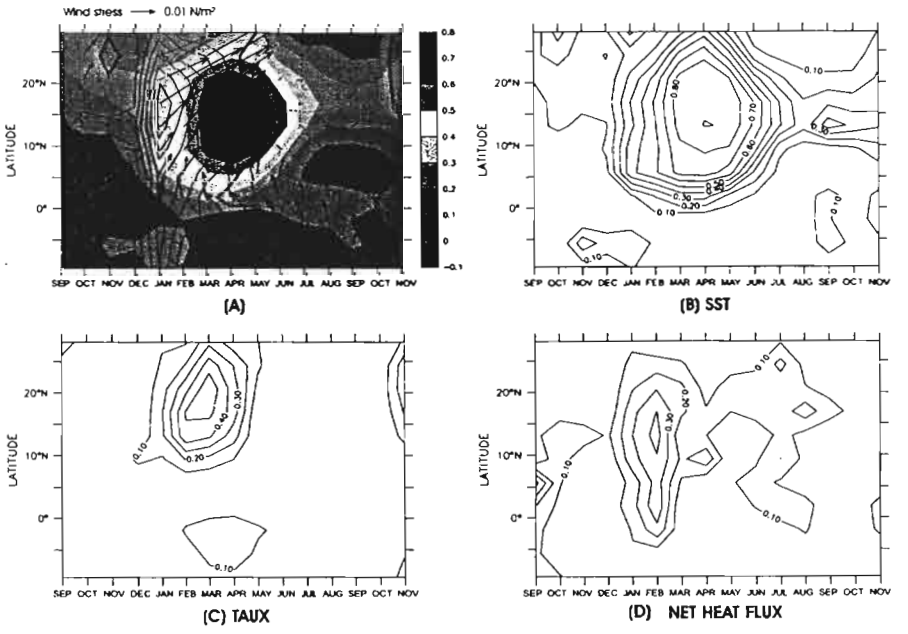

Figure D.1: Regressions of anomalies from ECMWF observations onto the NTASST index (A), Correlations of SST (B), TAUX (C), and net heat flux anomalies (D) with the NTASST index, over 19800–2000

After reproducing CVM's figure 2 (our figure 3.1) in (A) with different data, we have computed the Pearson's r^2 coefficient and displayed correlations between anomalies of SST, TAUX (zonal wind stress component), and net heat flux with the NTASST index.

SST On each map (figures D.1, D.2 and D.3), SST (Reynolds and Smith [1994]) are not modified. As expected, SST in the NTA region are very correlated to the NTASST index, especially between 5°N and 25°N, and around March-April-May, with correlations that peak 0.7 to 0.8.

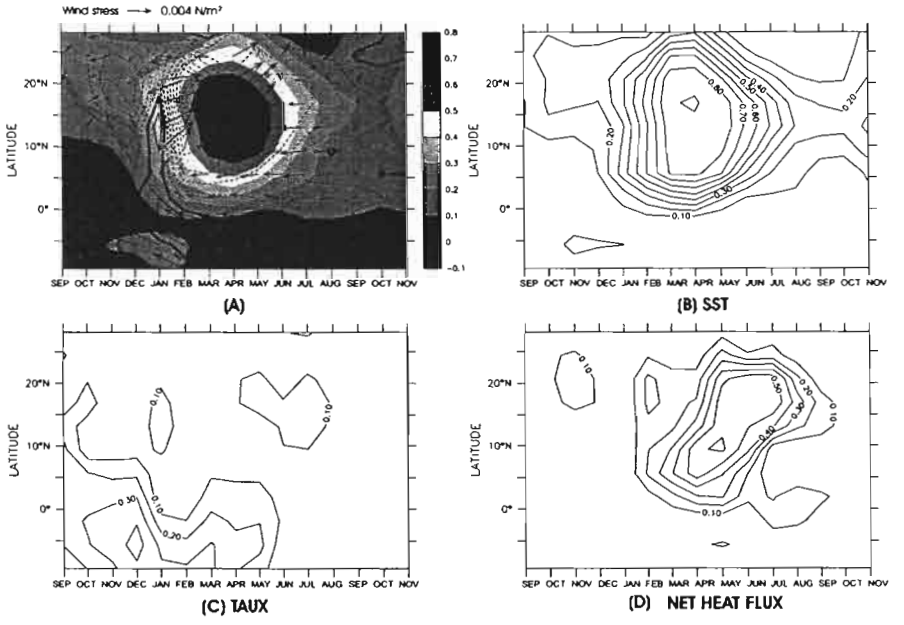

Figure D.2: Same as figure D.1, but for QTCM outputs from the «CONTROL» run, over the 1950-1999 period.

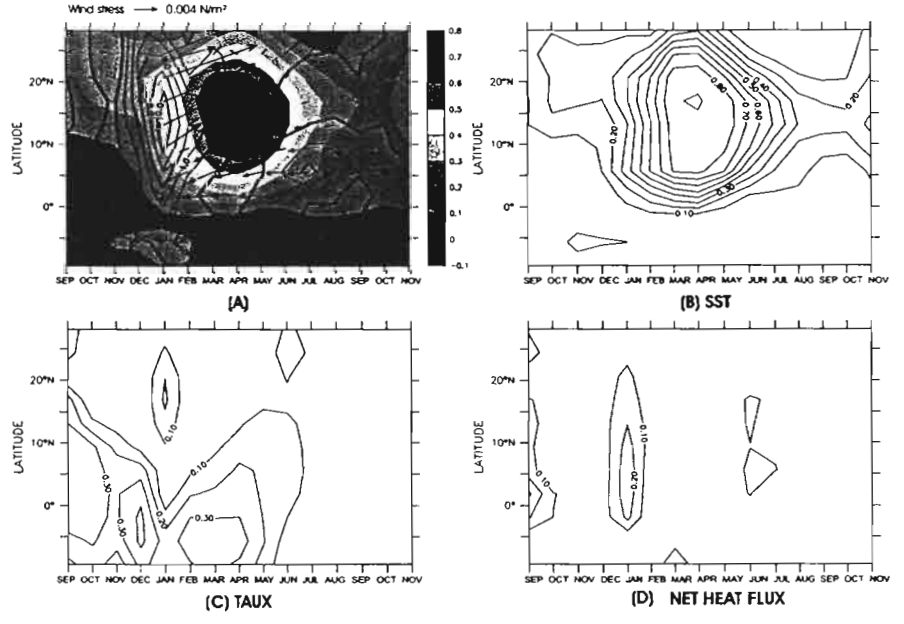

Figure D.3: Same as figure D.1 and D.2, but for QTCM outputs from the «PAC» run, over the 1950-1999 period.

Observations Figure D.1 displays the correlations of ECMWF data with the NTASST index. We find rather good correlations north of 5°N between TAUX anomalies and the NTASST index (up to 0.5), and north of 0°N between net heat flux anomalies and the NTASST index (up to 0.4). These relatively high correlations are located in January-February-March-April. It confirms that the mechanism leading to the SST anomalies is rather robust. However, zonal wind stress anomalies are very weak after April, so there

is no real correlation with the decrease of the NTASST after this date. Net heat negative flux anomalies are also weak after April (in comparaison with the positive anomalies), and the correlations after this date are too low (under 0.2) to link the decrease of the SST with evaporation losses.

QTCM outputs, «CONTROL» run Figure D.2 displays the correlations between anomalies from QTCM outputs from the «CONTROL» run and the NTTASST index, over 1950–1999. We find high correlations, of the order of 0.4, after March and north of 0°N between the net heat flux anomalies and the NTASST index. This confirms the fact, that, in QTCM, the local forcing plays an important role in the decrease of the SST. QTCM responds to the SST warming by evaporation losses that lead to negative net heat flux anomalies after April. Local forcing seems to surpass the remote forcing. So it is not surprising to get better correlations between the local SST anomalies and flux anomalies that are due to this local forcing. However, such high correlations do not appear in the observations. It means that the response of QTCM to local forcing is overestimated and/or that other phenomenons are hidden by this response.

QTCM outputs, «PAC» run Figure D.3 displays the correlations between anomalies from QTCM outputs from the «PAC» run and the NTASST index, over 1950–1999. We find significant correlations (greater than 0.1) around January and north of 10°N, confirming that in QTCM, ENSO plays a role in the warming of the SST in the NTA region. However, these correlations are low and do not last enough. They are low partly because not every NTA SST anomalous event is due to El Niño according to CVM (NAO plays a role too).

E An oceanographic cruise

E.1 Context

In July 2003, the laboratoire d'océanographie physique of the IRD of Nouméa carried out an oceanographic cruise around New Caledonia. At first a long mission of one month was planned. The laboratory was suposed to collect data up to 5000 m depth from New Caledonia (about 20°S) to 10°N, at 165°E. Problems with the winch that should have been used obliged the team to reprogram another mission.

A research topic in the laboratory is the South Equatorial Current (SEC); In particular, this current is supposed to strike New Caledonia on the eastern coast. Not many measurements have already been done to document the properties of this current near New Caledonia. As this current then strikes Australia, before coming back to the equator, climatic (wind, precipitations, cloud cover, heat flux) anomalies born around New Caledonia may play a role in the low frequency variability of ENSO. An oceanographic cruise has thus been carried out to document this topic.

E.2 Equipement and method

Figure E.1: L'Alis.

The ship used for this cruise is a former trawler, 28 m long, called «Alis» (fig. E.1). 5 scientifics were on board :

- Yves Gouriou : IRD de Noumea, supervisor of the mission
- Alexandre Ganachaud : IRD de Noumea, researcher
- David Varillon, IRD de Noumea, electronic engineer
- Gaël Alory : ATER, Université de Nouvelle Calédonie
- Pierre Labarbe, intern.

To look for the current and determine its properties, 60 stations were planned. On each station, a rosette goes to 1000 m depth in the sea. The rosette is equipped with a CTD (Conductivity Temperature Depth), a LADCP (Lowered Acoustic Doppler Current Profiler), and of bottles for samples of sea water at different depths. The probe is used to get pressure, temperature, salinity and oxygen continuous data from the sea surface to 1000 m. The LADCP compute currents in sending acoustic signals that reflect on particles in motion, given to Doppler effect. The samples of sea water enable to sample the probe for salinity and oxygen.

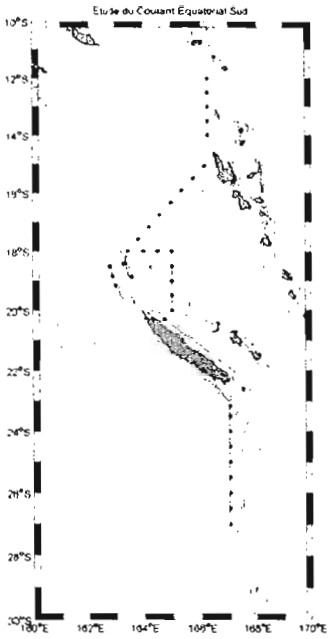

Figure E.2: Initial plan of the oceanographic cruise.

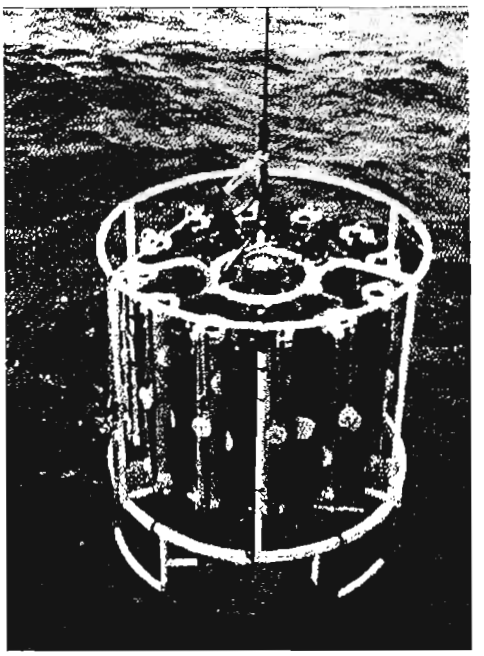

Figure E.3: The rosette with bottles for sea water samples. For our cruise, it was equipped with 6 bottles, a CTD probe, and a LADCP (not shown).

E.3 Results

Unfortunately, the weather was very bad during the cruise. Winds from 20 to 35 knots have blown almost all along the trip. The boat was too small for such a weather, and it was really dangerous to put the rosette in the sea, first for the sailors in charge of putting the probe in the water, and also for the probe itself (really expensive). Only 20 stations were done, in the North of New Caledonia, as far as Vanuatu. The results are not available yet, but some analysis show the existence

Acknowledgments

Quand on en arrive là, cela fleure bon la fin de rédaction... Ce n'est pas que ce travaille soit des plus pénible, rien n' a été vraiment pénible dans ces couloirs, mais une douce atmosphère de vacances se fait ressentir, ce qui n'est pas désagréable du tout. Voltaire, je vais à nouveau utiliser ta langue, si tu le permets.

Ces quelques mois en Calédonie auront été très enrichissants. Je remercie en premier lieu Boris, qui m'a permi de venir ici en m'offrant ce stage. Je ne sais pas si j'ai été à la hauteur, je ne sais pas si j'ai fait du bon boulot pour toi. Pour ma part, cela a été un plaisir de travailler avec toi. Je n'ai jamais stressé, tu m'as laissé bosser à mon rythme. La science dans ces conditions, c est parfait. Merci pour cette soirée dans ton luxeux appart. Dommage qu'il n'y en ait pas eu d'autre.

Merci à tout le labo aussi pour votre acceuil et votre aide, vos conseils éclairés, la mission en bateau : Yves, Alex, Gaël, Pierre, David, Francis (merci le hobbie cat!) Mansour (et son vélo), Jean-Michel et Jean-Marc. Mention spéciale à François, mon voisin de bureau, qui sait pourquoi.

Merci à tous ces sympathiques stagiaires, lofteurs et assimilés, collocataires ou voisins de bureau, thésards et VCAT de l'IRD, noble Institut de Relaxation et de Détente, avec qui j'ai passé ces six mois : mes océanographes et bien mangeurs/marcheurs Julien et Xavier, l'accent de Xavier et d'Eric, les facéties de Charles, la grande gueule de Greg, le sourire immuable d'Aurore, la jolie Julie, les yeux d'Enora, Christian, Nath, Tom, Barbara, Philipson mon premier colloc, Xavier, Tim, Ben, Guillaume, Guéno, Guillaume, les volleyeurs. Les autres qui viennent d'arriver, mais qui ne déméritent pas : Anaïs, Audrey, Berangère, Caroline, Kitty, Eric, Romain. Beaucoup de bons moments grâce a vous.

Merci aux cocotiers, au lagon, aux requins, aux dauphins, aux tortues. Aux gens de la CPS : Claire évidemment, ses collocs Phil et Scott, qui comprendront tout mon rapport sauf les remerciements, Marie-Ange et Sophie, Jackie... Ca fait pratiquer l'anglais.

Merci à mes surfers Niko et Lion, pour tout. Qu'aurait valu ce stage sans vous?

Scientifiquement parlant, ce stage aura également été bien instructif et très motivant. Malheureusement, la recherche en climatologie se résume bien souvent à faire de la programmation. Ca n'est pas ininteressant, cependant. C'était une bonne expérience. Le fait de travailler sur El Niño valide de toute manière tous ces travaux. J'ai apporté ma minuscule pierre à cet édifice, ça n'est pas si mal. J'en sais donc un peu plus à ce sujet, et j'en sais également un peu plus sur la place de la modélisation numérique. Ca n'est pas rien.

Océano, climato, météo, affaire à suivre? Who knows...

References

G Alory. *Redistribution zonale et méridienne de masse aux echelles ENSO et décennale dans le Pacifique Tropical.* PhD thesis, Université Paris VI, 2002.

B. Barnier, L. Siefridt, and P. Marchesiello. Thermal forcing for a global ocean circulation model using a three-year climatology of ECMWF analyses. *J. Marine Systems.*, pages 363–380, 1995.

F.P. Bretherton, R.E. Davis, and C.B. Fandry. A technique for objective analysis and design oceanographic experiments applied to mode-73. *Deep Sea*, 23:559–582, 1976.

S Cravatte. *El Niño and the Intraseasonal Waves in the Equatorial Pacific Ocean generated by the wind in the western part of the basin.* PhD thesis, Université Toulouse III, France, 2003.

A. Czaja, P. Van Der Vaart, and J. Marshall. A Diagnostic Study of the Role of Remote Forcing in Tropical Atlantic Variability. *J. Climate*, 15:3280–3290, 2002.

D.B. Enfield and A.M. Mestas-Nuñez. Global Mode of ENSO and Non-ENSO Sea Surace Temperature Variability and Their Associations with Climate. In *El Niño and the Southern Oscillation*, pages 89–112. Cambridge, 2000.

C.J. Hahn, S.G. Warren, and J. London. Edited synoptic cloud reports from ships and land stations over the globe, 1982–1991. DOE Rep. NDP02566B, 45pp. [Available from Carbon Dioxyde Information Analysis Center, Oak Ridge National Laboratory, P.O. Box 2008, Oak Ridge, TN 37831-6335], 1996.

E. Kalney and Coauthors. The NCEP/NCAR 40-Yer Reanalysis Project. *Bull. Meteor. Soc*, 77:437–471, 1996.

S.A. Klein, B. J. Soden, and Lau N.-C. Remote Sea Surface Temperature Variations during ENSO: Evidence for a Tropical Atmospheric Bridge. *J. Climate*, 12:917–932, 1999.

S. Levitus, T.P. Boyer, M.E. Conkright, T. O'Brien, J. Antonov, C. Stephens, L. Stathoplos, D. Johnson, and R. Gelfeld. World Ocean Database 1998 Volume 1: Introduction. NOAA Atlas NESDIS 18, U.S. Government Printing Office, Washington, D.C., 1998.

J.W-B. Lin, J.D. Neelin, and N. Zeng. Maintenance of Tropical Intraseasonal Variability: Impact of Evaporation-Wind Feedback and Midlatitude Storms. *J. Atmos. Sci.*, 57(17):2793–2823, 2000.

N.J. Mantua and S.R. Hare. The Pacific Decadal Oscillation. *Journal of Oceanography*, 58 (No.1):35–44, 2002.

J.D. Neelin and N. Zeng. A quasi-equilibrium tropical circulation model-formulation. *J. Atmos. Sci.*, 57: 1741–1766, 2000.

R.W. Reynolds and T.M. Smith. Improved global sea surface temperature analyses using optimum interpolation. *J. Climate*, 7:929–948, 1994.

H. Su, J.D. Neelin, and Chou.C. Tropical teleconnection and local response to SST anomalies during the 1997-1998 El Ninõ. *Journal of Geophysical Research*, 106:20,025–20,043, 2001.

K.E. Trenberth, D.P. Stepaniak, and J.W. Hurrel. Quality of reanalysis in the Tropics. *J. Climate*, 14: 1499–1510, 2001.

F. Vauclair and Y. du Penhoat. Interannual variability of the upper layer of the Atlantic Ocean from in situ data between 1979 and 1999. *Climate Dynamics*, 17:527–546, 2001.

N. Zeng, J.D. Neelin, and C. Chou. A quasi-equilibrium tropical circulation model-implementation and simulation. *J. Atmos. Sci.*, 57:1719–1736, 2000.